

# A Computational Framework for Evaluating the Role of Mobility on the Propagation of Epidemics on Point Processes

François Baccelli\* and Nithin Ramesan†

September 17, 2020

## Abstract

This paper is focused on SIS epidemic dynamics (also known as the contact process) on stationary Poisson point processes of the Euclidean plane, when the infection rate of a susceptible point is proportional to the number of infected points in a ball around it. Two models are discussed, the first with a static point process, and the second where points are subject to some random motion. For both models, we use conservation equations for moment measures to analyze the stationary point processes of infected and susceptible points. A heuristic factorization of the third moment measure is then proposed to derive simple polynomial equations allowing one to derive closed form approximations for the fraction of infected nodes and the steady state. These polynomial equations also lead to a phase diagram which tentatively delineates the regions of the space of parameters (population density, infection radius, infection and recovery rate, and motion rate) where the epidemic survives and those where there is extinction. According to this phase diagram, the survival of the epidemic is not always an increasing function of the motion rate. These results are substantiated by simulations on large two dimensional tori. These simulations show that the polynomial equations accurately predict the fraction of infected nodes when the epidemic survives. The phase diagram is also partly substantiated by the simulation of the mean survival time of the epidemic on large tori. The phase diagram accurately predicts the parameter regions where the mean survival time increases or decreases with the motion rate.

---

\*INRIA, France and UT Austin, USA

†UT Austin, USA

## Contents

<b>1</b>	<b>Introduction</b>	<b>3</b>
1.1	Basic Model and Aims . . . . .	4
1.2	Related Work . . . . .	6
1.2.1	The contact process on graphs . . . . .	6
1.2.2	The SIS epidemic on networks . . . . .	7
1.3	Structure of the Paper and Main Results . . . . .	8
<b>2</b>	<b>How to Use the Results</b>	<b>9</b>
2.1	Prediction of the stationary fraction of infected nodes . . . . .	9
2.2	Criticality Parameters and Tentative Phase Diagram . . . . .	10
2.3	Mathematical Tools and Simulation Methodology . . . . .	10
<b>3</b>	<b>Preliminaries</b>	<b>12</b>
3.1	Factorial Moment Measures and Pair Correlation Functions . . . . .	12
3.1.1	Definition . . . . .	12
3.1.2	A General Relation between Pair Correlation Functions . . . . .	13
3.2	Graphical Representation . . . . .	13
<b>4</b>	<b>First Moment RCP</b>	<b>16</b>
4.1	General Formulation . . . . .	16
4.2	A Necessary Condition for Survival . . . . .	17
4.3	Reformulation in Terms of Moment Measures . . . . .	18
<b>5</b>	<b>Far Random Waypoint Motion Model</b>	<b>19</b>
5.1	RCP for Second Moment Measure . . . . .	20
5.2	Heuristics on Third Moment Measures . . . . .	22
5.2.1	Heuristics based on Bayes' formula and conditional independence . . . . .	23
5.2.2	Heuristics based on means . . . . .	24
5.2.3	Combinations . . . . .	25
5.2.4	Classification . . . . .	26
5.3	Terminology for Functional and Polynomial Equations . . . . .	30
5.3.1	Heuristic B1I . . . . .	31
5.3.2	Heuristic B1G1 . . . . .	31
5.3.3	Heuristic M2BI . . . . .	32
5.3.4	Heuristic $M_{\infty}BI$ . . . . .	33
5.3.5	Heuristic $M_{\infty}BG1$ . . . . .	34
5.4	Numerical Results . . . . .	34

5.5	A Tentative Phase Diagram . . . . .	34
5.6	Critical Values . . . . .	37
5.6.1	M2BI . . . . .	37
5.6.2	B1I . . . . .	40
5.7	Simulation Validation . . . . .	43
5.7.1	Stationary densities . . . . .	43
5.7.2	Comparison of heuristics . . . . .	45
5.7.3	Simulation close to criticality . . . . .	45
<b>6</b>	<b>No-Motion Case</b>	<b>51</b>
6.1	Rate Conservation Principle for Intensities . . . . .	52
6.2	Second Moment RCP . . . . .	53
6.3	Heuristics . . . . .	55
6.3.1	Heuristic B1I . . . . .	56
6.3.2	Heuristic G1 . . . . .	57
6.3.3	Heuristic B1G1 . . . . .	57
6.3.4	Heuristic M2BI . . . . .	58
6.3.5	Heuristic $M_{\infty}BI$ . . . . .	59
6.3.6	Heuristic $M_{\infty}BG1$ . . . . .	61
6.4	Numerical Results . . . . .	61
6.4.1	Densities . . . . .	61
6.4.2	Pair correlation functions . . . . .	62
<b>7</b>	<b>Variants</b>	<b>62</b>
7.1	Epidemic Model Variants . . . . .	62
7.2	Far Random Waypoint and Death . . . . .	63
<b>8</b>	<b>List of Conjectures</b>	<b>65</b>
<b>9</b>	<b>Appendix</b>	<b>65</b>
9.1	On the Far Random Waypoint Model . . . . .	65
9.2	On the Boolean Cluster above Percolation . . . . .	69
9.3	Mean Time between Two Infections . . . . .	70

## 1 Introduction

This paper is focused on the use of the theory of point processes for the analysis of the propagation of an epidemic and of the policies to control it, in particular the reduction of individual motion.

The general framework is that of a stochastic SIS (Susceptible, Infected, Susceptible) model on point processes of the Euclidean plane. In SIS, each individual has a state which is either Susceptible or Infected. It moves from  $S$  to  $I$  upon infection by another individual. From  $I$ , it moves to  $S$  after after some recovery time. Below we will use the terms SIS process and contact process equivalently.

The model considered here is stochastic in several distinct ways:

1. The individuals are located at the points of a random point process on  $\mathbb{R}^2$ , which accounts for the random geometry of the problem, and in particular the fact that at any given time, the epidemic propagates more easily in more densely populated areas;
2. The individuals have some parameterizable random motion, which accounts for the randomness of displacement and allows one to study the effect of mobility reduction;
3. The infection process itself is a random phenomenon that takes into account the geometry of the configuration of other individuals around a susceptible node through a shot-noise of the configuration of infected nodes, which allows one to incorporate the specificity of and the randomness in the contagion scheme.

## 1.1 Basic Model and Aims

There is initially a single point process  $\Xi_0$ , which will here be Poisson homogeneous of intensity  $\lambda$  in the Euclidean plane, representing the initial location of individuals. Points move independently.

We will consider the following *far random waypoint motion model* where at any time, a point stays put for an exponential time and jumps from its current location to another location with rate  $\gamma$ ; the displacements are random, i.i.d., independent, and have a symmetrical distribution  $D$  on  $\mathbb{R}^2$ . This leads to a location point process  $\Xi_t$  at time  $t$ . Note that  $\Xi_t$  is Poisson with intensity  $\lambda$  for all  $t$  thanks to the displacement theorem.

There is an interaction/contagion/viral charge function  $f : \mathbb{R}^+ \rightarrow \mathbb{R}^+$ . The special case

$$f(r) = \alpha 1_{r \leq a}$$

will be considered in the analysis. In this function,  $\alpha > 0$  is the pairwise infection rate and  $a > 0$  is the infection radius. In words, the rate at which a susceptible node is infected is proportional to the number of infected nodes that are at distance less than  $a$  from it. More general functions (with bounded or unbounded support) can be considered in the theory and in the computational analysis.

The points of  $\Xi_t$  can be in one of two states: 1 (or infected) or 0 (or susceptible). This leads to two point processes

$$\Xi_t = \Phi_t + \Psi_t,$$

with  $\Phi_t$  (resp.  $\Psi_t$ ) the point process of infected (resp. susceptible) individuals. The SIS state dynamics is then as follows:

- At any time, the state of a susceptible point jumps to infected with a rate equal to the current value of the shot-noise w.r.t.  $f$  (sum of viral charges) at its current location. That is, the transition rate of  $X \in \Psi_t$  is

$$a(X, \Phi_t) = \sum_{Y \in \Phi_t} f(\|X - Y\|).$$

This accounts for the geographic locality of the infection mechanism, i.e., the higher chance of infection when surrounded by more infected individuals.

- At any time, the state of an infected point jumps to susceptible with a constant rate  $\beta > 0$ .

This comes in addition to motion.

In all cases described above, the pair  $(\Phi_t, \Psi_t)$  is Markov on the space of counting measures, which is not a discrete space.

Here is another and equivalent representation of the basic model in terms of a countable collection of state processes. Number the points of  $\Xi_0$  with the integers. Associate a piecewise constant, left continuous stochastic process  $S_i(t)$ , with state space  $\{0, 1\}$ , to point  $i$ , with 0 for susceptible and 1 for infected. For each  $i$ , the transition rates from one state to the other are time-point processes with certain stochastic intensities. The stochastic intensity of transitions of the state of node  $i$  from 1 to 0 is

$$b_i(t, \omega) = \beta 1_{S_i(t)=1}. \quad (1)$$

Let  $V_i(t)$  denote the displacement of point  $i$  of  $\Xi$  at time  $t$ . This random variable depends on the motion model. The position of point  $i$  at time  $t$  is hence

$$X_i(t) = X_i(0) + V_i(t).$$

Let

$$I_{i, \Phi(t)} = I_{\Phi(t)}(X_i(t)) = \sum_{j \neq i} f(\|X_i(t) - X_j(t)\|) 1_{S_j(t)=1}$$

denote the infection rate seen by node  $i$  at time  $t$ , whatever its current state. The stochastic intensity of transitions of the state of node  $i$  from 0 to 1 is

$$a_i(t, \omega) = I_{i, \Phi(t)} 1_{S_i(t)=0}. \quad (2)$$

If there is no-motion, we have a countable collection of coupled Markov chains with transition rates

$$b_i(t, \omega) = \beta 1_{S_i(t)=1} \quad (3)$$

and

$$a_i(t, \omega) = \left( \sum_{j \neq i} f(\|X_i(0) - X_j(0)\|) 1_{S_j(t)=1} \right) 1_{S_i(t)=0}. \quad (4)$$

The general aim of this paper is to study the role of motion on the equilibria. The equilibria in question are mostly studied in the *infinite Euclidean plane*, which allows one to leverage the machinery of stationary point processes.

In these infinite models, for each equilibrium, we are interested in the density of infected nodes in the steady state, the mean time between two infections, etc. There are also more fundamental questions such as the existence of equilibria and the identification of the phase diagram, namely critical values of the parameters separating regions where the epidemic a.s. dies out or has a positive probability to survive.

## 1.2 Related Work

Previous work related to this paper broadly falls into two categories: the interacting particle system literature (in particular the literature on the contact process on graphs) and the mathematical epidemiology literature (in particular the literature on SIS epidemic over networks). In this work, we leverage the mathematical machinery that draws from the former body of literature. The heuristics we propose to estimate quantities of interest are linked to those considered in the latter body of work.

### 1.2.1 The contact process on graphs

In the absence of mobility, the problem was extensively studied in the particle system literature (see [4] and references therein). A basic dichotomy in this framework is between finite and infinite graphs. On finite graphs, the main question is that of the phase transition between a logarithmic and an exponential growth of the time till absorption. This was studied on deterministic graphs like finite grids and regular trees. There is a large corpus of results on infinite graphs such as grids and

regular trees. This is well covered in the book of T. Liggett [4]. The main results bear on the monotonicity and the so-called self-duality of the propagation process. These properties allow one to prove important structural results like (i) the existence of a critical value on the infection rate above which the epidemic survives with a positive probability and below which it almost surely disappears, whatever the initial conditions; (ii) the existence of a maximal invariant measure which is that obtained when starting from the situation where all nodes are infected. The contact process was also studied on infinite random graphs with unbounded degrees. It was first studied on the supercritical Bienaymé-Galton-Watson tree [7] where it was shown that some critical values can be degenerate. Contact process models on Euclidean point processes were also thoroughly studied (see ex. [10], [11], [12]). The case without motion of the present paper can be seen as the contact process on the random geometric graph.

### 1.2.2 The SIS epidemic on networks

Epidemics on networks have also been extensively studied. The focus here is on computationally tractable approaches allowing one to predict relevant epidemiological quantities and to derive qualitative properties of the epidemic. [6] provides a comprehensive overview of methods and literature on the topic. In particular, the infinite collection of moment measure equations and subsequent heuristics described in Section 5.2 are similar in spirit to methods used in this literature for the analysis of SIS epidemics on (non-geometric, finite) graphs (see Section V.A in [6] and chapter 17 of [13]). Epidemics with motion were extensively studied in the random graph setting (without considering geometry). The basic model for SIS on graphs is that where agents perform a random walk on the random graph and where agents meeting at a give node of the graph may infect each other - see [5] and the references therein.

In the present paper, we focus on a point process model with the following motion: a point stays at a given location for an exponential time and then makes a jump with a large magnitude. This is inspired by the idea of a flight. We are not aware of previous research on previous studies on SIS epidemics on point processes with motion. The main difference with the literature on random geometric graphs is the fact that the structure of the random geometric graph evolves randomly over time in the case studied in the present paper, whereas it is fixed in [11] and the other references mentioned. Further, we derive accurate heuristics for quantities of interest, unlike most of the work in the interacting particle systems literature. The main difference with the literature on SIS epidemics on networks is that we explicitly model the effects of the geometry of the contact graph using the theory

of point processes.

In summary, the novelty of this paper is that it considers both the effects of the geometry that is inherent to populations affected by epidemics *and* the effects of population motion, while deriving computational heuristics that describe the consequences of these effects.

### 1.3 Structure of the Paper and Main Results

Section 2 contains a summary on how the proposed framework can be used in practice without entering the mathematical background nor the proof techniques.

Section 3 is meant to provide an introduction to the point process and particle system techniques used in the paper. It contains in particular the proof of structural results like monotonicity and self duality which can be extended to this case by techniques similar to those in [4]. This is used to show that for both the no-motion and motion cases, there exists a threshold on  $\beta$  (equivalently  $\alpha$ ),  $\beta_c$  (equivalently  $\alpha_c$ ) such that the epidemic dies out for  $\beta > \beta_c$  (equivalently  $\alpha < \alpha_c$ ) and survives otherwise - to use epidemiological terms, we show the existence of an *epidemic threshold*.

Section 4 uses the rate conservation principle (RCP) on intensities (first moment measures). This allows one to derive a necessary condition for the existence of a non degenerate stationary regime (here non-degenerate means with a positive density of infected nodes) and a general Palm relation between the stationary density of infected nodes and the pair correlation functions of infected and susceptible nodes. This leads to a conjecture (Lemma 2) on the value of the epidemic threshold.

Section 5 discusses the random waypoint model alluded to above in the special case where a point stays fixed for an exponential random time of parameter  $\gamma$  and then makes a large jump. It contains the RCP equations satisfied by moment measures of the stationary infected and susceptible point processes. It also contains a detailed description of the heuristic factorization of third moment measures which lead to the polynomial equations alluded to above. This leads to heuristic evaluations of the fraction  $p$  of infected nodes in the stationary regime of the epidemic process (which is known as the *endemic disease state* in the epidemiology literature).  $p$  is also equal to the probability that a single infected individual will cause a sustained epidemic. This also leads to a tentative phase diagram (see Fig. 1) that partitions the space of parameters  $(\alpha, \beta, \gamma, \lambda, a)$  into regions of survival and extinction of the epidemic.

Section 6 uses the same methodology to analyze the case without motion.

Section 7 discusses variants of practical importance to which the techniques of the present paper should be applicable.



Finally, Section 8 gathers the list of conjectures that are made throughout the paper.

## 2 How to Use the Results

### 2.1 Prediction of the stationary fraction of infected nodes

Assume one wants to predict the fraction  $p$  of nodes that are infected in the steady state when there is survival. Note that by self-duality, this is also the probability that a single infected node leads to an epidemic that survives.

Let us illustrate through one example among several others discussed in Section 5 how to use some polynomial heuristic to do this. Let  $w$  be the value of the pair-correlation function at distance zero of the infected and susceptible point processes. The intuitive meaning of  $w$  is as follows: given that there is a susceptible point at the origin, the intensity of infected points in the near vicinity of the origin (near is understood w.r.t.  $a$ ) is not  $\lambda p$  as it would be if there was no probabilistic dependence between infected and susceptible, but  $\lambda p w$  with  $w < 1$ . Then, we show that for each one of the heuristic factorizations in question, the unknown variable  $w$  satisfies some explicit polynomial equation that practically allow one to characterize it and  $p$  in closed form. For instance, for a certain factorization based on Bayes' rule (see Subsection 5.3.3),  $w$  is a positive number satisfying

$$(2\gamma + \beta)((\alpha\mu w - \beta + 2\gamma)(w^2\alpha^2\mu^2 - 2\beta(\alpha\mu w - \beta)w) + w(\alpha\mu w - \beta)\beta^2 - 2\gamma\beta^2) \\ = (\alpha\mu w - \beta)(\alpha\mu w - \beta + 2\gamma)(2\gamma(\alpha\mu w - \beta) + 2\alpha\beta w + \beta w(\alpha\mu w - \beta)), \quad (5)$$

where  $\gamma$  is the motion rate,  $\beta$  the recovery rate,  $\alpha$  the infection rate, and  $\mu = \lambda\pi a^2$ , with  $\lambda$  the spatial intensity of the Poisson point process and  $a$  is the infection radius. Once  $w$  is determined through this polynomial equation,  $p$  is then obtained through the formula

$$p = 1 - \frac{\beta}{\alpha\mu w}. \quad (6)$$

Discrete event simulation of the dynamics over large tori shows that the solution of this polynomial equation allows one to accurately predict the fraction of infected nodes as announced. Each factorization gives slightly different numerical results, as is natural for different heuristics, but always in line with the simulation results.

Section 6 uses the same methodology to analyze the case without motion. If there is no percolation of the Boolean model of radius  $a$  on a PPP with intensity  $\lambda$ , then, although all Boolean clusters are finite, there are arbitrarily large clusters far away, and the epidemic might persist for a long time in these large clusters. However, the epidemic dies out in a.s. finite time in all Boolean clusters intersecting

any finite domain. Hence in this case, the only steady state is that with no infected nodes.

## 2.2 Criticality Parameters and Tentative Phase Diagram

Each of these polynomial equations also leads to a phase diagram determining the regions of the parameter space where there is survival or extinction. The boundaries between these regions are characterized by stating that  $p = 0$  in the last polynomial system. This leads to further polynomial relations between the  $(\mu, \gamma, \alpha, \beta)$  parameters. More precisely, this leads to the identification of a *safe region*, where there is extinction whatever the motion rate  $\gamma$ , a region which is *unsafe and motion-insensitive*, namely such that there is survival for all positive motion rates, and a region which is *unsafe and motion-sensitive*. This last region is the most surprising: when fixing all parameters except  $\gamma$ , there are two thresholds  $0 < \gamma_c^- < \gamma_c^+$  such that there is survival for  $\gamma < \gamma_c^-$  and for  $\gamma > \gamma_c^+$  and extinction for  $\gamma_c^- < \gamma < \gamma_c^+$ . In other words, we find that, for certain subsets of the parameter space, a reduction in the motion of the population can be favorable to the propagation of the epidemic. The general shape of the phase diagram is depicted in Figure 1. The precise definitions of the boundaries between the regions again slightly vary depending on the chosen heuristic. The general structure is nevertheless common to all the considered heuristics.

Since this phase diagram is based on the polynomial heuristics, it is itself a heuristic. Its qualitative validity could not be proved within the framework of this paper. We explain in Subsection 5.7.3 how it can be partially substantiated by simulation on large tori. In particular, it is shown that, on any large torus, when picking a  $\mu$  and a  $\beta$  in the unsafe motion-insensitive region, the mean time to extinction sharply increases with motion rate in the vicinity of  $\gamma_c^-$  and sharply decreases with this rate in the vicinity of  $\gamma_c^+$ . These monotonicity properties can be substantiated by simulation using confidence intervals on this mean time to extinction. In addition to partially substantiating the phase diagram (which deals with epidemics living on the infinite plane), these simulation results also show that the phase diagram accurately predicts the trends of the survival time of the epidemic when it lives on a large finite torus. An important observation suggested both by the phase diagram and simulation is that decreasing motion rate *does not always result in the epidemic dying out more quickly*.

## 2.3 Mathematical Tools and Simulation Methodology

The machinery of particle systems [4] will be leveraged to prove structural results on the model, and in particular to assess basic monotonicity properties and the ex-

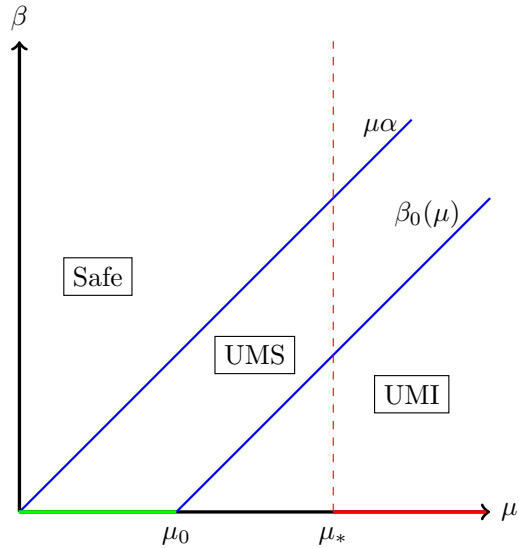


Figure 1: The  $(\mu, \beta)$ -phase diagram. Region UMI is the unsafe, motion-insensitive region. Region UMS is the unsafe, motion-sensitive region. The region delimited by red semi-line (on the right of  $\mu_* \sim 4.5$ ) is the Boolean supercritical region where there is survival in the no-motion case. The green segment, on the left of  $\mu_0 \sim 0.34$ , is the motion-subcritical region which is the set of values of  $\mu$  where there UMI region is empty. The blue segment is the motion-supercritical, Boolean-subcritical subset of  $\mu$ .

istence of critical values for certain parameters. Graphical analysis is instrumental in proving that, for both models, when fixing all parameters except  $\alpha$ , there is a critical value of  $\alpha$ , say  $\alpha_c$ , above which the epidemic survives with a positive probability and below which it dies out with probability 1. In particular, self-duality shows that a positive probability of survival is equivalent to having the maximal invariant measure of the contact process being non-degenerate (i.e., with a positive fraction of infected nodes). Extinction is equivalent to having the empty measure being the only stationary regime of the SIS dynamics.

The quantitative analysis of the paper is based on conservation equations satisfied by stationary factorial moment measures of the infected and susceptible point processes (Lemma 1 and Theorem 3 for the motion case, Lemma 8 and Theorem 9 for the motionless case). Mean field models are also be used in order to derive further computational results when the motion rate is high. The analysis is based on the rate conservation principle of Palm calculus [1] and is inspired from that

developed in [2] and [8]. We could not solve these conservation equations which are in terms of an infinite hierarchy of functional equations. It is why we introduce the approximation alluded to above which consists in truncating this hierarchy of equations. This truncation is based on a heuristic factorization of third moment measures in terms of the first two moment measures which is described in Subsection 5.2. This heuristic leads to a fixed point integral equation for the moment measures of orders one and two (or equivalently the intensities and pair correlation functions) of these point processes, which in turn leads to the announced polynomial equations (Subsection 5.3 for the motion case and Subsection 6.3 for the motionless case). The equations are quite different in the motion and motionless cases and they require different mathematical settings. In the no-motion case, the best results will be obtained when working on the so-called infinite cluster, whereas there is no such object in the case with motion where the results will be obtained when working on the whole Poisson point process. They will have different qualitative properties: for instance, assume that the Boolean (or random connection) model of the initial condition does not percolate; in the no-motion case, the epidemic dies out for sure (in the sense that the steady state has no infected node in any finite window) for all (non degenerate) values of the SIS parameters; however, there are fast motion scenarios for which there exist (non-degenerate) values of the SIS parameters for which the epidemic survives.

A discrete event simulator was developed to empirically analyze the SIS dynamics over point processes (with and without motion) on large tori. The quantitative results obtained by the integral and polynomial equations are compared with the statistics obtained from the discrete event simulator in a systematic way. These comparisons are distributed in the analysis sections. Simulation at criticality, namely for parameter regions where the epidemic is on the edge of extinction, is computationally challenging.

### 3 Preliminaries

#### 3.1 Factorial Moment Measures and Pair Correlation Functions

##### 3.1.1 Definition

The second factorial moment measure of a point process  $\phi$ ,  $\rho_\phi^{(2)}$ , is defined by

$$\mathbb{E}\left[\sum_{X \neq X' \in \phi} g(X, X')\right] = \int_{\mathbb{R}^2} g(x, x') \rho_\phi^{(2)}(x, x') dx dx',$$

for all measurable non-negative functions  $g$ . For a stationary point process of intensity  $\lambda$ ,

$$\rho_\phi^{(2)}(x, x') = \lambda^2 \xi_\phi^{(2)}(x' - x),$$

with  $\xi_\phi$  the correlation function of  $\phi$ .

Similarly, the joint moment measure of  $(\phi, \psi)$ ,  $\rho_{\phi, \psi}^{(2)}$ , is defined by

$$\mathbb{E} \left[ \sum_{X \in \phi, Y \in \psi} g(X, Y) \right] = \int_{\mathbb{R}^2} g(x, y) \rho_{\phi, \psi}^{(2)}(x, y) dx dy,$$

for all measurable non-negative functions  $g$ . In the case of two jointly (space)-stationary point processes with intensities  $\lambda$  and  $\mu$ ,

$$\rho_{\phi, \psi}^{(2)}(x, x') = \lambda \mu \xi_{\phi, \psi}^{(2)}(x' - x),$$

with  $\xi_{\phi, \psi}^{(2)}$  the pair correlation function of  $(\phi, \psi)$ .

In the isotropic case, we have

$$\xi_{\phi, \psi}^{(2)}(x' - x) = \tilde{\xi}_{\phi, \psi}^{(2)}(\|x' - x\|).$$

By abuse of notation, we will often drop the tilde in the RHS of the last relation.

### 3.1.2 A General Relation between Pair Correlation Functions

Let  $(v, \phi, \psi)$  be three jointly stationary point processes such that  $v = \phi + \psi$ . Let  $\lambda, \mu$  be the intensities of  $\phi$  and  $\psi$ , respectively. Let  $p = \lambda/(\lambda + \mu)$ . Then, for all  $r$ ,

$$(1 - p)^2 \xi_{\psi, \psi}^{(2)}(r) + p^2 \xi_{\phi, \phi}^{(2)}(r) + 2p(1 - p) \xi_{\psi, \phi}^{(2)}(r) = \xi_{v, v}^{(2)}(r). \quad (7)$$

where the RHS will depend on the fact that  $v$  is, e.g., a clustered or a repulsive point process. If  $\phi + \psi$  forms a Poisson point process, then

$$(1 - p)^2 \xi_{\psi, \psi}^{(2)}(r) + p^2 \xi_{\phi, \phi}^{(2)}(r) + 2p(1 - p) \xi_{\psi, \phi}^{(2)}(r) = 1. \quad (8)$$

In what follows, we will use the simplified notation  $\xi_{\psi, \psi}(r)$  in place of  $\xi_{\psi, \psi}^{(2)}(r)$  for the pair correlation function of  $(\phi, \psi)$ .

## 3.2 Graphical Representation

**Deterministic graphs** For the SIS dynamics (or contact process) on a fixed graph  $\Xi$ , the following results are obtained from the graphical representation of the dynamics [4]. In these results, for all  $A \subset \Xi$ ,  $\Phi_t^A$  denotes the subset of infected nodes of  $\Xi$  at time  $t$  if the set of infected nodes at time 0 is  $A$ . In the coupling of the graphical representation of the dynamics, we have

- Monotonicity:

$$\text{if } A \subset B, \text{ then } \Phi_t^A \subset \Phi_t^B, \text{ for all } t.$$

- Additivity:

$$\Phi_t^{A \cup B} = \Phi_t^A \cup \Phi_t^B, \text{ for all } A, B, t.$$

- Self-duality

$$\mathbb{P}^A(\Phi_t \cap B \neq \emptyset) = \mathbb{P}^B(\Phi_t \cap A \neq \emptyset), \text{ for all } A, B, t.$$

A direct consequence of monotonicity is the existence of a maximal (time) invariant measure which is obtained as the limiting measure when starting with all nodes infected. The existence of this limiting measure follows from the fact that the state measure is stochastically decreasing over time for this initial condition.

A useful consequence of self-duality is the fact that the probability that the epidemic survives when started from singleton  $\{x\}$ , with  $x \in \Xi$ , namely

$$\lim_{t \rightarrow \infty} \mathbb{P}^{\{x\}}(\Phi_t \cap \Xi \neq \emptyset),$$

coincides with the mass of the maximal time-invariant probability measure at  $x$ , namely

$$\lim_{t \rightarrow \infty} \mathbb{P}^\Xi(\Phi_t \cap \{x\} \neq \emptyset).$$

One says that there is strong survival if, for some  $x$ , for the initial condition  $\{x\}$ ,  $x$  is infected infinitely often with positive probability. One says that there is survival if for some  $x$ , the probability that the total number of infected nodes is non-zero for all  $t$  is positive. If there is survival but no strong survival, one speaks of weak survival. The most general structural result on the contact process states that when all parameters are fixed except  $\alpha$ , there are two thresholds on  $\alpha$ ,  $0 \leq \alpha_1 \leq \alpha_2 \leq \infty$  such that if  $\alpha < \alpha_1$ , the epidemic dies out, if  $\alpha_1 < \alpha < \alpha_2$ , there is weak survival of the epidemic, and there is strong survival if  $\alpha > \alpha_2$ . This is a consequence of monotonicity. Note that one can also fix all parameters except  $\beta$  and get a similar result that there exist  $0 \leq \beta_2 \leq \beta_1 \leq \mu$  such that if  $\beta > \beta_1$ , the epidemic dies out, if  $\beta_2 < \beta < \beta_1$ , there is weak survival, and there is strong survival if  $\beta < \beta_2$ .

In the present paper, we concentrate on strong survival (survival will always mean strong survival). If the probability that the epidemic strongly survives when started from  $\{x\}$  is positive for some  $\alpha$ , then it is positive for all  $\alpha' > \alpha$  and for all  $x$ . Hence there exists a critical  $\alpha_c$  (not depending on  $x$ ) such that for all  $\alpha < \alpha_c$ , the epidemic dies out almost surely when starting from  $x$ , and when  $\alpha > \alpha_c$ , it (strongly) survives with a positive probability.

**Random geometric graph** In case the graph is random, the basic properties listed above hold conditionally on the graph topology. If the graph is a random geometric graph of a stationary and ergodic point process  $\Xi$  under its Palm distribution, if  $\mathcal{F}$  denotes the sigma algebra generated by  $\Xi$ , then

$$\mathbb{P}^{\{x\}}(\Phi_\infty \cap \Xi \neq \emptyset \mid \mathcal{F}) = \mathbb{P}^\Xi(\Phi_\infty \cap \{x\} \neq \emptyset \mid \mathcal{F}), \quad \text{for all } t.$$

When letting  $t$  tend to infinity, one gets that the (conditional) maximal time stationary measure on the random discrete set  $\Xi$  puts a mass at  $x \in \Xi$  equal to the (conditional) probability that the epidemic started at  $x$  survives.

By unconditioning w.r.t.  $\mathcal{F}$ , one gets

$$\mathbb{P}_0(\Phi_\infty \cap \Xi \neq \emptyset \mid \Phi_0 = \{0\}) = \mathbb{P}_0(\Phi_\infty \cap \{0\} \neq \emptyset \mid \Phi_0 = \Xi),$$

where  $\mathbb{P}_0$  is the Palm probability of the point process  $\Xi$ . The LHS is the probability that the epidemic survives when started from the typical point (the origin) or equivalently the spatial average of the probability of survival starting from a single point. The RHS is the probability that the origin is infected in the maximal stationary regime, or equivalently the fraction of infected nodes in a large ball under this maximal stationary regime.

Also, there exists a constant (this is a constant because of ergodicity)  $\alpha_c$  such that for  $\alpha < \alpha_c$ , the epidemic dies out when started from any point of the point process (or equivalently the maximal invariant measure is 0), whereas it survives with a positive probability otherwise (or equivalently the conditional maximal invariant random measure is positive a.s.).

Note that, due to ergodicity, if the origin is infected i.o. with positive probability, it is with probability 1.

**Random geometric graph with node motion** Assume now that there is motion in the random waypoint sense defined above. Namely, at times given by an exponential clock with rate  $\gamma$ , a node jumps to another location keeping its SIS state. Then, whenever the displacements are according to a smooth symmetrical distribution  $D$  (e.g. Gaussian centered independent per dimension), the three basic properties (monotonicity, additivity, and self-duality) based on the graphical representation can be extended to this case. The proof leverages a space-time random graph whose state at time  $t$  consists of the positions of the particles at that time. Each particle stays put for an exponential time and then jumps from its position to a new one (obtained by adding an independent random variable with distribution  $D$ ). This graph being given, one proceeds as in the basic graphical representation by adding potential recovery epochs and pairwise infection epochs on this space-time graph. Given an initial SIS state of the nodes, one then extends the notion of

causal infection path of the classical case to this case of node motion. The proof of the desired properties are then obtained from the following facts: (i) the space-time random graph is infinite and has a single connected component (this follows from fact that for all pairs of points, the first time at which they are at distance less than  $a$  is a.s. finite due to the recurrence of the associated random walk in  $\mathbb{R}^2$ ) (ii) the directed paths in the associated space-time graphical representations are still “reversible”, which is instrumental in extending self-duality. So all the conclusions extend to this case as well. In particular, there exists a critical  $\alpha_c$  (or equivalently  $\beta_c$ ), there exists a maximal invariant measure, etc.

**Random geometric graph with far random waypoint motion** The far random waypoint model studied in the present paper belongs to the class discussed above when displacements are large. A natural instance is that of a two dimensional Gaussian vector with i.i.d. coordinates  $\mathcal{N}(0, \sigma^2)$  with  $\sigma^2$  large. It is proved in Appendix 9.1 that in the steady state, if the fraction of infected nodes is  $p$ , then, when  $\sigma$  is large, the point processes  $(\mathcal{I}, \mathcal{S})$  of arrivals of infected and susceptible points after  $t$  are both close to space-time Poisson, with  $\mathcal{I}$  and  $\mathcal{S}$  independent,  $\mathcal{I}$  of intensity  $\lambda p \gamma$ ,  $\mathcal{S}$  of intensity  $\lambda(1-p)\gamma$ , and  $(\mathcal{I}, \mathcal{S})$  independent of  $\{(\Phi_s, \Psi_s)\}_{s \leq t}$ . This will be instrumental in the following.

## 4 First Moment RCP

### 4.1 General Formulation

Assume that there exists a time-space stationary regime for the dynamics (with or without motion). Let  $p$  denote the (unknown) stationary fraction of infected nodes. That is, in this stationary regime,  $\Phi_t$  has spatial intensity  $\lambda p$  and  $\Psi_t$  has intensity  $\lambda(1-p)$ .

Let

$$I_{\Phi_t}(x) = \sum_{X \in \Phi_t} f(\|X - x\|)$$

denote the infection rate of locus  $x \in \mathbb{R}^2$  at time  $t$ . The time-space stationary assumption and Campbell’s formula imply

$$\mathbb{E}[I_{\Phi_t}(x)] = \lambda p F,$$

with

$$F = 2\pi \int_0^\infty f(r) r dr.$$

In the special case (assumed here by default),  $F = \pi a^2 \alpha$ .



Pick a subset  $D$  of the Euclidean space with volume 1. The spatial infection rate is defined as

$$i = \mathbb{E}\left[\sum_{Y \in \Psi_t \cap D} I_{\Phi_t}(Y)\right].$$

From Campbell's formula

$$i = \lambda(1-p)\mathbb{E}_{\Psi}^0[I_{\Phi(0)}],$$

with  $(\Phi, \Psi)$  representatives of the time-space stationary point processes and  $\mathbb{E}_{\Psi}^0$  the Palm distribution w.r.t.  $\Psi$ .

The spatial recovery rate is defined as

$$r = \mathbb{E}\left[\sum_{X \in \Phi_t \cap D} \beta\right] = \lambda p \beta.$$

The RCP gives that  $i = r$ , namely

**Lemma 1.** *Under the foregoing assumptions,*

$$p\beta = (1-p)\mathbb{E}_{\Psi}^0[I_{\Phi(0)}]. \quad (9)$$

The last relation will be referred to as the *first moment RCP*.

## 4.2 A Necessary Condition for Survival

A natural conjecture, strongly backed by simulations, is that there is repulsion between  $\Phi$  and  $\Psi$ , namely

$$\mathbb{E}_{\Psi}^0[I_{\Phi(0)}] \leq \mathbb{E}[I_{\Phi(0)}].$$

In words, in the steady state, a typical susceptible individual will see less infection than a typical locus in space. This will be referred to as the *repulsion conjecture*.

This and Lemma 1 give

$$p\beta = (1-p)\mathbb{E}_{\Psi}^0[I_{\Phi(0)}] \leq (1-p)p\mu,$$

that is, if  $p \neq 0$ ,

$$p \leq 1 - \frac{\beta}{\alpha\mu},$$

with

$$\mu = \lambda\pi a^2$$

the mean degree in the random geometric graph. This proves the following result on the critical values  $\alpha_c$  and  $\beta_c$  defined in Section 3.2:

**Lemma 2.** *Under the  $(\Phi, \Psi)$  repulsion conjecture,*

$$\alpha_c \geq \frac{\beta}{\mu}, \quad \beta_c \leq \alpha\mu. \quad (10)$$

This lemma is conditional on the conjecture. It can be rephrased as follows: if  $\alpha < \frac{\beta}{\mu}$ , there is extinction (in that the only invariant measure is the empty measure), whereas if  $\alpha > \frac{\beta}{\mu}$ , then there is survival (in that the maximal invariant measure is non degenerate, or equivalently that probability that the epidemic survives starting from a single infected individual is positive). In addition either  $p = 0$  or the fraction of infected nodes satisfies

$$0 < p \leq 1 - \frac{\beta}{\alpha\mu}. \quad (11)$$

Note that motion plays no role in this lemma. It is in fact hidden in the Palm expectation. Also note that the result holds for all stationary point processes (we did not use the Poisson assumption here). This will be used in the next subsection.

The thresholds stated in Lemma 2 can be connected to the basic reproduction number ( $\mathcal{R}_0$ ) from epidemiology. This number is defined as the expected number of infections generated by a single infected individual located in a population of all-susceptible individuals. In epidemiology, an emerging infection is predicted to spread in a population if  $\mathcal{R}_0$  is greater than 1 in most models. Since a single infected individual has average degree  $\mu$ , infects neighbours at rate  $\alpha$  and recovers at rate  $\beta$ , it is easy to see that at least in the fast motion case,  $\mathcal{R}_0 = \frac{\alpha\mu}{\beta}$ . The condition

$$\mathcal{R}_0 = \frac{\alpha\mu}{\beta} > 1,$$

is exactly the conjecture in Lemma 2.

### 4.3 Reformulation in Terms of Moment Measures

It is possible to represent the Palm expectation used above in terms of moment measures. We have

$$\mathbb{E}_{\Psi}^0[I_{\Phi(0)}] = \lambda p \int_{\mathbb{R}^2} f(x) \xi_{\Phi, \Psi}(x) dx.$$

So (9) can be rephrased in terms of the following integral equation:

$$\beta = (1 - p) \lambda \int_{\mathbb{R}^2} \xi_{\Psi, \Phi}(x) f(\|x\|) dx. \quad (12)$$

If the correlation function  $\xi_{\Psi, \Phi}(\cdot)$  is constant equal to 1, which is the case when  $\Phi$  and  $\Psi$  are independent (possibly in the infinite velocity case), then this boils down to

$$\beta = \alpha(1 - p)\mu, \quad (13)$$

that is

$$p = 1 - \frac{\beta}{\alpha\mu}, \quad (14)$$

assuming that  $\frac{\beta}{\alpha\mu} < 1$ . In other words, if there exists a non-degenerate stationary regime with  $\Phi$  and  $\Psi$  independent, then this achieves the upper bound in (11). We conjecture that this regime is achieved in the high velocity case provided  $\alpha\mu > \beta$ , which is backed by simulations.

Let us come back to the general case for  $\xi_{\Psi, \Phi}$ . If we take the special case discussed above for  $f$ , we get

$$\beta = (1 - p)\lambda\alpha \int_{B(0, a)} \xi_{\Psi, \Phi}(x) dx.$$

Repulsion between  $\Phi$  and  $\Psi$  implies that

$$\int_{B(0, a)} \xi_{\Psi, \Phi}(x) dx \leq \pi a^2.$$

So for fixed  $a, \alpha, \beta, \lambda$ , any model with repulsion requires a smaller  $p$  than the infinite velocity (or fast motion mean-field) model, which is in line with the bound in (11).

One can use isotropy to write (12) as

$$\lambda p \beta = \lambda(1 - p)\lambda p 2\pi \int_{\mathbb{R}^+} \xi_{\Psi, \Phi}(r) f(r) r dr. \quad (15)$$

Note the abuse of notation: we used the same notation as above for the pair correlation functions in polar coordinates.

## 5 Far Random Waypoint Motion Model

The far random waypoint model features a mix of zero velocity and far away motion. Each point has an independent exponential clock with rate  $\gamma$ . When its clock ticks, the point jumps very far away. Arrivals are hence according to a Poisson rain with intensity  $\lambda\gamma p$  for type I and independent Poisson rain of rate  $\lambda\gamma(1 - p)$  for type  $S$ .

We recall the structural results listed in Section 3.2: assume all parameters fixed except  $\alpha$ . There exists  $\alpha_c$  such that for  $\alpha < \alpha_c$ , the epidemic dies out for sure (or equivalently the maximal invariant measure is the zero measure), whereas for  $\alpha > \alpha_c$  the epidemic survives with a positive probability (or equivalently the maximal invariant measure is a positive measure). Here is another possible formulation: assume all parameters fixed except  $\beta$ . There exists  $\beta_c$  such that for  $\beta > \beta_c$ , the epidemic dies out for sure (or equivalently the maximal invariant measure is the zero measure), whereas for  $\beta < \beta_c$  the epidemic survives with a positive probability (or equivalently the maximal invariant measure is a positive measure).

Note that we do not know whether there exists a similar threshold on the parameter  $\gamma$ . At first glance, motion seems instrumental in the propagation of the epidemic by bringing infected nodes from far away (this is particularly true when there is no Boolean-percolation in the model without motion). However, motion may also dissolve dense clusters where the epidemic survives for an arbitrarily long time. This is an important mathematical question, to which the tentative phase diagram obtained in this section gives a somewhat unexpected answer: in the present setting, motion is not always favoring the survival of the epidemic.

### 5.1 RCP for Second Moment Measure

One can see the LHS of the first moment RCP equation (9) as the "mass birth rate" of  $\rho_{\Psi}^{(1)}$  (or equivalently the mass death rate of  $\rho_{\Phi}^{(1)}$ ) and the RHS as the "mass death rate" of  $\rho_{\Psi}^{(1)}$  (or equivalently the mass birth rate of  $\rho_{\Phi}^{(1)}$ ). We see that this conservation law on the first moment measure involves a second moment measure.

One can think in the same terms for second moment measures. Let  $\mu(\Phi)_{\Psi, \Phi}^{0,r}(x)$  denote the conditional density of  $\Phi$  at  $x$  given that  $\Psi$  has a points at  $(0, 0)$  and  $\Phi$  a point at  $(r, 0)$ . Let also  $\mu(\Phi)_{\Psi, \Psi}^{0,r}(x)$  denote the conditional density of  $\Phi$  at  $x$  given that  $\Psi$  has a points at  $(0, 0)$  and a point at  $(r, 0)$ . The main result of this section is

**Theorem 3.** *Under the far random waypoint mobility model with jump rate  $\gamma$ , if there exists a stationary regime, then the stationary pair correlation functions satisfy*

the following system of integral equations:

$$\begin{aligned}
p\xi_{\Phi,\Phi}(r)(\beta + \gamma) &= p\gamma \\
&+ (1-p)\xi_{\Psi,\Phi}(r) \left( f(r) + \int_{\mathbb{R}^2} \mu(\Phi)_{\Psi,\Phi}^{0,r}(x) f(\|x\|) dx \right) \\
p\xi_{\Psi,\Phi}(r)\beta + (1-p)\gamma &= (1-p)\xi_{\Psi,\Psi}(r) \left( \gamma + \int_{\mathbb{R}^2} \mu(\Phi)_{\Psi,\Psi}^{0,r}(x) f(\|x\|) dx \right) \\
\beta &= \lambda(1-p)2\pi \int_{\mathbb{R}^+} \xi_{\Psi,\Phi}(r) f(r) r dr \\
1 &= (1-p)^2\xi_{\Psi,\Psi}(r) + p^2\xi_{\Phi,\Phi}(r) - 2p(1-p)\xi_{\Psi,\Phi}(r).
\end{aligned} \tag{16}$$

*Proof.* The last equation comes from the fact that  $\Xi_t$  is Poisson.

Here is a sketch of the proof for the other equations.

The "mass birth rate" in  $\rho_{\Phi,\Phi}^{(2)}(r)$  is

$$2\lambda p \lambda p \gamma + 2\rho_{\Psi,\Phi}^{(2)}(r) \left( f(r) + \int_{\mathbb{R}^2} \mu(\Phi)_{\Psi,\Phi}^{0,r}(x) f(\|x\|) dx, \right)$$

where we used the fact that arrivals of infected nodes are Poisson of intensity  $\lambda\gamma p$  (see the end of Subsection 3.2). and the "mass death rate" in  $\rho_{\Phi,\Phi}^{(2)}(r)$  is

$$2\rho_{\Phi,\Phi}^{(2)}(r)(\beta + \gamma).$$

The 2 comes from the fact that the recovery of motion of a point of  $\Phi$  deletes two infected points at a distance  $r$  of each other. The "mass death rate" in  $\rho_{\Phi,\Phi}^{(2)}(r)$  is

$$\begin{aligned}
p^2\xi_{\Phi,\Phi}(r)(\beta + \gamma) &= p^2\gamma \\
&+ p(1-p)\xi_{\Psi,\Phi}(r) \left( f(r) + \int_{\mathbb{R}^2} \mu(\Phi)_{\Psi,\Phi}^{0,r}(x) f(\|\mathbf{x}\|) d\mathbf{x} \right).
\end{aligned} \tag{17}$$

□

Note that if  $\gamma = 0$ , then (17) boils down to

$$p\xi_{\Phi,\Phi}(r)\beta = (1-p)\xi_{\Psi,\Phi}(r) \left( f(r) + \int_{\mathbb{R}^2} \mu(\Phi)_{\Psi,\Phi}^{0,r}(x) f(\|\mathbf{x}\|) d\mathbf{x} \right)$$

which is (82).

Similarly, the "mass birth rate" in  $\rho_{\Psi,\Psi}^{(2)}(r)$  is

$$2\rho_{\Psi,\Phi}^{(2)}(r)\beta + 2\lambda^2(1-p)^2\gamma,$$

and the "mass death rate" in  $\rho_{\Psi,\Psi}^{(2)}(r)$  is

$$2\rho_{\Psi,\Psi}^{(2)}(r) \left( \gamma + \int_{\mathbb{R}^2} \mu(\Phi)_{\Psi,\Psi}^{0,r}(\mathbf{x}) f(\|\mathbf{x}\|) d\mathbf{x} \right).$$

Hence

$$\begin{aligned} & p(1-p)\xi_{\Psi,\Phi}(r)\beta + (1-p)^2\gamma \\ &= (1-p)^2\xi_{\Psi,\Psi}(r) \left( \gamma + \int_{\mathbb{R}^2} \mu(\Phi)_{\Psi,\Psi}^{0,r}(\mathbf{x}) f(\|\mathbf{x}\|) d\mathbf{x} \right). \end{aligned} \tag{18}$$

For  $\gamma = 0$ , we find back (83) in Section 6. Similarly, if  $\xi \equiv 1$ , this leads to (13).

Assume that when  $\gamma \rightarrow \infty$ , there is a finite limit for each  $\xi$  function. Then (17) implies that, when  $\gamma$  tends to infinity,  $\xi_{\Phi,\Phi}(r)$  tends to 1 for all  $r$ . By the same argument used on (18), one gets that, when  $\gamma$  tends to infinity,  $\xi_{\Psi,\Psi}(r)$  tends to 1 for all  $r$ . Hence, from (8),  $\xi_{\Psi,\Psi}(r)$  tends to 1 for all  $r$  as well. But we know that for such pair correlation functions, the relation (13)

$$\beta = (1-p)\alpha\mu$$

holds. In this sense, the last equations give the desired continuum between the no velocity and the high velocity cases.

## 5.2 Heuristics on Third Moment Measures

Note that the last theorem provides a conservation law on second moment measures which involves third moment measures. One can of course go along the path that now consists in writing down a conservation law for third moment measures which will involve moment measures of order four and so on. This infinite hierarchy of integral equations (which was discussed in a different context in [2]) should characterize the dynamics in an exact way. We will rather go on a more computational path by considering the heuristics of the next subsection.

This path consists in introducing various factorization heuristics for third moment measures. Each of them leads to a system of integral equations jointly satisfied by the first and second order moment measures, which in turn provide computational approximations for these measures.

The heuristics in question are of two types: either based on Bayes' formula and a conditional independence approximation, or based on a simple form of conditional dependence.

### 5.2.1 Heuristics based on Bayes' formula and conditional independence

Below, we describe various heuristics which are all based on a conditional independence approximation and can be summarized as follows: the  $\mu$  densities defined above are conditional densities of infected points at  $\mathbf{x} \in \mathbb{R}^2$  given the two events, e.g. that there is a susceptible point at  $\mathbf{0} = (0, 0)$  and another susceptible point at  $\mathbf{r} := (r, 0)$ . We use Bayes' formula to represent this in terms of the conditional probability that there is a susceptible point at  $\mathbf{0}$  and another susceptible point at  $\mathbf{r}$  given there is an infected point at  $\mathbf{x}$ . We then use the conditional independence approximation to represent the latter in terms of a product of pair correlation functions.

Consider first  $\mu(\Phi)_{\Psi, \Psi}^{\mathbf{0}, \mathbf{r}}(\mathbf{x})$ , which we recall to be the conditional density of  $\Phi$  at  $x$  under the two point Palm probability of  $\Psi$  at  $(0, 0)$  and  $(0, r)$ . Denote by  $\mu(\Psi, \Phi)_{\Psi}^{\mathbf{r}}(0, x)$  the joint density of  $(\Psi, \Phi)$  at  $(\mathbf{0}, \mathbf{x})$  under the Palm of  $\Psi$  at  $\mathbf{r}$  and use a similar notation for  $\mu(\Psi, \Phi)_{\Psi}^{\mathbf{0}}(\mathbf{r}, \mathbf{x})$  and  $\mu(\Psi, \Psi)_{\Phi}^{\mathbf{x}}(\mathbf{0}, \mathbf{r})$ . The third moment density of  $(\Psi, \Psi, \Phi)$  at  $(\mathbf{0}, \mathbf{r}, \mathbf{x})$  is

$$\mu(\Phi)_{\Psi, \Psi}^{\mathbf{0}, \mathbf{r}}(\mathbf{x}) \xi_{\Psi, \Psi}(\mathbf{r}) \lambda^2 (1-p)^2$$

and we have the following conditional representations of the latter:

$$\begin{aligned} \mu(\Phi)_{\Psi, \Psi}^{\mathbf{0}, \mathbf{r}}(\mathbf{x}) \xi_{\Psi, \Psi}(\mathbf{r}) \lambda^2 (1-p)^2 &= \mu(\Psi, \Psi)_{\Phi}^{\mathbf{x}}(\mathbf{0}, \mathbf{r}) \lambda p \\ &= \mu(\Psi, \Phi)_{\Psi}^{\mathbf{r}}(\mathbf{0}, \mathbf{x}) \lambda (1-p) \\ &= \mu(\Psi, \Phi)_{\Psi}^{\mathbf{0}}(\mathbf{r}, \mathbf{x}) \lambda (1-p), \end{aligned}$$

which is in essence Bayes' rule rewritten in three different ways.

For three jointly stationary point processes  $\pi$ ,  $\phi$ , and  $\psi$ , let  $\rho_{\phi, \psi, \pi}^{(3)}(x, y, z)$  denote the the third moment density of  $(\phi, \psi, \pi)$  at  $(x, y, z)$ . The use of Bayes' rule is heuristically justified when interpreting

$$\rho_{\phi, \psi, \pi}^{(3)}(x, y, z) \Delta x \Delta y \Delta z$$

as the probability that  $\phi$  has one point in a small neighborhood of  $x$  of volume  $\Delta x$ ,  $\psi$  has one point in a small neighborhood of  $y$  of volume  $\Delta y$ , and  $\pi$  has one point in a small neighborhood of  $z$  of volume  $\Delta z$ .

So for all positive integers  $k$  and  $l$ ,

$$\begin{aligned} &\left( \mu(\Phi)_{\Psi, \Psi}^{\mathbf{0}, \mathbf{r}}(\mathbf{x}) \xi_{\Psi, \Psi}(\mathbf{r}) \lambda^2 (1-p)^2 \right)^{k+2l} \\ &= \left( \mu(\Psi, \Psi)_{\Phi}^{\mathbf{x}}(\mathbf{0}, \mathbf{r}) \lambda p \right)^k \left( \mu(\Psi, \Phi)_{\Psi}^{\mathbf{r}}(\mathbf{0}, \mathbf{x}) \lambda (1-p) \right)^l \left( \mu(\Psi, \Phi)_{\Psi}^{\mathbf{0}}(\mathbf{r}, \mathbf{x}) \lambda (1-p) \right)^l \\ &= \left( \xi_{\Psi, \Phi}(\|\mathbf{x}\|) \lambda (1-p) \xi_{\Psi, \Phi}(\|\mathbf{x} - \mathbf{r}\|) \lambda (1-p) \lambda p \right)^k \\ &\quad \left( \xi_{\Psi, \Psi}(\mathbf{r}) \lambda (1-p) \xi_{\Psi, \Phi}(\|\mathbf{x} - \mathbf{r}\|) \lambda p \lambda (1-p) \right)^l \\ &\quad \left( \xi_{\Psi, \Psi}(\mathbf{r}) \lambda (1-p) \xi_{\Psi, \Phi}(\|\mathbf{x}\|) \lambda p \lambda (1-p) \right)^l, \end{aligned}$$

where the last relation follows from the conditional independence heuristic.

The meaning of  $k$  and  $l$ , which will be used for the classification below, is the following: a bigger  $k$  puts in some sense more emphasis on the positive correlation structure.

It follows that

$$\mu(\Phi)_{\Psi, \Psi}^{\mathbf{0}, \mathbf{r}}(\mathbf{x}) = \lambda p \xi_{\Psi, \Phi}(\|\mathbf{x}\|)^{\frac{k+l}{k+2l}} \xi_{\Psi, \Phi}(\|\mathbf{x} - \mathbf{r}\|)^{\frac{k+l}{k+2l}} \xi_{\Psi, \Psi}(r)^{-\frac{k}{k+2l}}. \quad (19)$$

Similarly

$$\begin{aligned} & \left( \mu(\Phi)_{\Psi, \Phi}^{\mathbf{0}, \mathbf{r}}(\mathbf{x}) \xi_{\Psi, \Phi}(r) \lambda^2 (1-p)p \right)^{k+2l} \\ &= (\mu(\Psi, \Phi)_{\Phi}^{\mathbf{x}}(\mathbf{0}, \mathbf{r}) \lambda p)^l (\mu(\Psi, \Phi)_{\Phi}^{\mathbf{r}}(\mathbf{0}, \mathbf{x}) \lambda p)^l (\mu(\Phi, \Phi)_{\Psi}^{\mathbf{0}}(\mathbf{r}, \mathbf{x}) \lambda (1-p))^k \\ &= (\xi_{\Psi, \Phi}(\|\mathbf{x}\|) \lambda (1-p) \xi_{\Phi, \Phi}(\|\mathbf{x} - \mathbf{r}\|) \lambda p \lambda p)^l \\ & \quad (\xi_{\Psi, \Phi}(r) \lambda (1-p) \xi_{\Phi, \Phi}(\|\mathbf{x} - \mathbf{r}\|) \lambda p \lambda p)^l \\ & \quad (\xi_{\Psi, \Phi}(r) \lambda p \xi_{\Psi, \Phi}(\|\mathbf{x}\|) \lambda p \lambda (1-p))^k. \end{aligned}$$

Hence

$$\mu(\Phi)_{\Psi, \Phi}^{\mathbf{0}, \mathbf{r}}(\mathbf{x}) = \lambda p \xi_{\Psi, \Phi}(\|\mathbf{x}\|)^{\frac{k+l}{k+2l}} \xi_{\Phi, \Phi}(\|\mathbf{x} - \mathbf{r}\|)^{\frac{2l}{k+2l}} \xi_{\Psi, \Phi}(r)^{-\frac{l}{k+2l}}. \quad (20)$$

### 5.2.2 Heuristics based on means

Consider first  $\mu(\Phi)_{\Psi, \Phi}^{\mathbf{0}, \mathbf{r}}(\mathbf{x})$ , which we recall to be the conditional density of  $\Phi$  at  $x$  under the two point Palm probability of  $\Psi$  at  $(0, 0)$  and  $\Phi$  at  $(0, r)$ . Heuristically this, multiplied by  $\Delta x$ , is the probability of event  $A$  that there is a point in a region of small volume  $\Delta x$  around  $x$  given two events  $B$  and  $C$ , that is  $P(A | B \cap C)$ . The only data we have are  $P(A | B)$  and  $P(A | C)$ . A natural heuristic is the geometric mean

$$P(A | B \cap C) \sim \sqrt{P(A | B)P(A | C)}.$$

A more general heuristic is

$$P(A | B \cap C) \sim P(A | B)^\eta P(A | C)^{1-\eta},$$

with  $0 \leq \eta \leq 1$ . One can also consider the arithmetic mean

$$P(A | B \cap C) \sim \frac{P(A | B) + P(A | C)}{2}.$$

A more general heuristic is

$$P(A | B \cap C) \sim P(A | B)\eta + P(A | C)(1-\eta),$$



with  $0 \leq \eta \leq 1$ .

The geometric mean leads to

$$\mu(\Phi)_{\Psi, \Psi}^{\mathbf{0}, \mathbf{r}}(\mathbf{x}) = \lambda p \xi_{\Psi, \Phi}(\|\mathbf{x}\|)^\eta \xi_{\Psi, \Phi}(\|\mathbf{x} - \mathbf{r}\|)^{1-\eta} \quad (21)$$

and

$$\mu(\Phi)_{\Psi, \Phi}^{\mathbf{0}, \mathbf{r}}(\mathbf{x}) = \lambda p \xi_{\Psi, \Phi}(\|\mathbf{x}\|)^\eta \xi_{\Phi, \Phi}(\|\mathbf{x} - \mathbf{r}\|)^{1-\eta}. \quad (22)$$

Note that a bigger  $\eta$  puts more emphasis on the positive correlation.

The arithmetic mean leads to

$$\mu(\Phi)_{\Psi, \Psi}^{\mathbf{0}, \mathbf{r}}(\mathbf{x}) = \lambda p (\eta \xi_{\Psi, \Phi}(\|\mathbf{x}\|) + (1 - \eta) \xi_{\Psi, \Phi}(\|\mathbf{x} - \mathbf{r}\|)) \quad (23)$$

and

$$\mu(\Phi)_{\Psi, \Phi}^{\mathbf{0}, \mathbf{r}}(\mathbf{x}) = \lambda p (\eta \xi_{\Psi, \Phi}(\|\mathbf{x}\|) + (1 - \eta) \xi_{\Phi, \Phi}(\|\mathbf{x} - \mathbf{r}\|)). \quad (24)$$

Here, a bigger  $\eta$  puts more emphasis on the negative correlation.

### 5.2.3 Combinations

In the Bayes' approach, one can replace the conditional independence step by the mean heuristic. For the geometric mean case, this leads to

$$\begin{aligned} & \left( \mu(\Phi)_{\Psi, \Psi}^{\mathbf{0}, \mathbf{r}}(\mathbf{x}) \xi_{\Psi, \Psi}(r) \lambda^2 (1-p)^2 \right)^{k+2l} \\ &= \left( \mu(\Psi, \Psi)_{\Phi}^{\mathbf{x}}(\mathbf{0}, \mathbf{r}) \lambda p \right)^k \left( \mu(\Psi, \Phi)_{\Psi}^{\mathbf{r}}(\mathbf{0}, \mathbf{x}) \lambda (1-p) \right)^l \left( \mu(\Psi, \Phi)_{\Psi}^{\mathbf{0}}(\mathbf{r}, \mathbf{x}) \lambda (1-p) \right)^l \\ &= \left( \xi_{\Psi, \Phi}(\|\mathbf{x}\|) \lambda (1-p) \sqrt{\xi_{\Psi, \Phi}(\|\mathbf{x} - \mathbf{r}\|) \xi_{\Psi, \Psi}(r) \lambda (1-p) \lambda p} \right)^k \\ & \quad \left( \sqrt{\xi_{\Psi, \Psi}(r) \xi_{\Psi, \Phi}(\|\mathbf{x}\|) \lambda (1-p) \xi_{\Psi, \Phi}(\|\mathbf{x} - \mathbf{r}\|) \lambda p \lambda (1-p)} \right)^l \\ & \quad \left( \sqrt{\xi_{\Psi, \Psi}(r) \xi_{\Psi, \Phi}(\|\mathbf{x} - \mathbf{r}\|) \lambda (1-p) \xi_{\Psi, \Phi}(\|\mathbf{x}\|) \lambda p \lambda (1-p)} \right)^l \end{aligned}$$

and

$$\begin{aligned}
& \left( \mu(\Phi)_{\Psi, \Phi}^{\mathbf{0}, \mathbf{r}}(\mathbf{x}) \xi_{\Psi, \Phi}(r) \lambda^2 (1-p)p \right)^{k+2l} \\
&= \left( \mu(\Psi, \Phi)_{\Phi}^{\mathbf{x}}(\mathbf{0}, \mathbf{r}) \lambda p \right)^l \left( \mu(\Psi, \Phi)_{\Phi}^{\mathbf{r}}(\mathbf{0}, \mathbf{x}) \lambda p \right)^l \left( \mu(\Phi, \Phi)_{\Psi}^{\mathbf{0}}(\mathbf{r}, \mathbf{x}) \lambda (1-p) \right)^k \\
&= \left( \xi_{\Psi, \Phi}(\|\mathbf{x}\|) \lambda (1-p) \sqrt{\xi_{\Phi, \Phi}(\|\mathbf{x} - \mathbf{r}\|) \xi_{\Psi, \Phi}(r) \lambda p \lambda p} \right)^l \\
&\quad \left( \xi_{\Psi, \Phi}(r) \lambda (1-p) \sqrt{\xi_{\Phi, \Phi}(\|\mathbf{x} - \mathbf{r}\|) \xi_{\Psi, \Phi}(\|\mathbf{x}\|) \lambda p \lambda p} \right)^l \\
&\quad \left( \xi_{\Psi, \Phi}(r) \lambda p \sqrt{\xi_{\Psi, \Phi}(\|\mathbf{x}\|) \xi_{\Phi, \Phi}(\|\mathbf{x} - \mathbf{r}\|) \lambda p \lambda (1-p)} \right)^k.
\end{aligned}$$

The rationale is as above. This now leads to

$$\mu(\Phi)_{\Psi, \Psi}^{\mathbf{0}, \mathbf{r}}(\mathbf{x}) = \lambda p \xi_{\Psi, \Phi}(\|\mathbf{x}\|)^{\frac{k+3l/2}{k+2l}} \xi_{\Psi, \Phi}(\|\mathbf{x} - \mathbf{r}\|)^{\frac{k/2+3l/2}{k+2l}} \xi_{\Psi, \Psi}(r)^{-\frac{l+k/2}{k+2l}} \quad (25)$$

and

$$\mu(\Phi)_{\Psi, \Phi}^{\mathbf{0}, \mathbf{r}}(\mathbf{x}) = \lambda p \xi_{\Psi, \Phi}(\|\mathbf{x}\|)^{\frac{k/2+3l/2}{k+2l}} \xi_{\Phi, \Phi}(\|\mathbf{x} - \mathbf{r}\|)^{\frac{l+k/2}{k+2l}} \xi_{\Psi, \Phi}(r)^{-\frac{l/2}{k+2l}}. \quad (26)$$

#### 5.2.4 Classification

**Bayes Independent** Here are a few special cases to be used below and named using the value of the ratio  $l/k$ . We recall that a smaller ratio emphasizes the positive correlation (that between  $\Psi$  and  $\Psi$  or that between  $\Phi$  and  $\Phi$ , whereas a bigger ratio emphasizes the negative correlation between  $\Phi$  and  $\Psi$ .

- Heuristic B0I (Bayes 0 Independent) is for  $k = \infty$  (maximal emphasis on negative correlation) and conditional independence:

$$\mu(\Phi)_{\Psi, \Psi}^{\mathbf{0}, \mathbf{r}}(\mathbf{x}) = \lambda p \frac{\xi_{\Psi, \Phi}(\|\mathbf{x}\|) \xi_{\Psi, \Phi}(\|\mathbf{x} - \mathbf{r}\|)}{\xi_{\Psi, \Psi}(r)} \quad (27)$$

and

$$\mu(\Phi)_{\Psi, \Phi}^{\mathbf{0}, \mathbf{r}}(\mathbf{x}) = \lambda p \xi_{\Psi, \Phi}(\|\mathbf{x}\|), \quad (28)$$

where we see that the influence of the susceptible at  $\mathbf{r}$  is ignored.

- Heuristic B1I corresponds to  $l = k = 1$  (equal emphasis on positive and negative correlations) and conditional independence:

$$\mu(\Phi)_{\Psi, \Psi}^{\mathbf{0}, \mathbf{r}}(\mathbf{x}) = \lambda p \frac{\xi_{\Psi, \Phi}(\|\mathbf{x}\|)^{\frac{2}{3}} \xi_{\Psi, \Phi}(\|\mathbf{x} - \mathbf{r}\|)^{\frac{2}{3}}}{\xi_{\Psi, \Psi}(r)^{\frac{1}{3}}} \quad (29)$$

and

$$\mu(\Phi)_{\Psi, \Phi}^{\mathbf{0}, \mathbf{r}}(\mathbf{x}) = \lambda p \frac{\xi_{\Psi, \Phi}(\|\mathbf{x}\|)^{\frac{2}{3}} \xi_{\Phi, \Phi}(\|\mathbf{x} - \mathbf{r}\|)^{\frac{2}{3}}}{\xi_{\Psi, \Phi}(r)^{\frac{1}{3}}}. \quad (30)$$

- Heuristic  $B_{\frac{1}{2}}I$  corresponds to  $2l = k = 1$  (variant of the latter with a bit more emphasis on negative correlation) and conditional independence:

$$\mu(\Phi)_{\Psi, \Psi}^{\mathbf{0}, \mathbf{r}}(\mathbf{x}) = \lambda p \frac{\xi_{\Psi, \Phi}(\|\mathbf{x}\|)^{\frac{3}{4}} \xi_{\Psi, \Phi}(\|\mathbf{x} - \mathbf{r}\|)^{\frac{3}{4}}}{\xi_{\Psi, \Psi}(r)^{\frac{1}{2}}}. \quad (31)$$

and

$$\mu(\Phi)_{\Psi, \Phi}^{\mathbf{0}, \mathbf{r}}(\mathbf{x}) = \lambda p \frac{\xi_{\Psi, \Phi}(\|\mathbf{x}\|)^{\frac{3}{4}} \xi_{\Phi, \Phi}(\|\mathbf{x} - \mathbf{r}\|)^{\frac{1}{2}}}{\xi_{\Psi, \Phi}(r)^{\frac{1}{4}}}. \quad (32)$$

- Heuristic  $B_{\infty}I$  is for  $l = \infty$  (all emphasis on positive correlations) and conditional independence:

$$\mu(\Phi)_{\Psi, \Psi}^{\mathbf{0}, \mathbf{r}}(\mathbf{x}) = \lambda p \xi_{\Psi, \Phi}(\|\mathbf{x}\|)^{\frac{1}{2}} \xi_{\Psi, \Phi}(\|\mathbf{x} - \mathbf{r}\|)^{\frac{1}{2}} \quad (33)$$

and

$$\mu(\Phi)_{\Psi, \Phi}^{\mathbf{0}, \mathbf{r}}(\mathbf{x}) = \lambda p \frac{\xi_{\Psi, \Phi}(\|\mathbf{x}\|)^{\frac{1}{2}} \xi_{\Phi, \Phi}(\|\mathbf{x} - \mathbf{r}\|)}{\xi_{\Psi, \Phi}(r)^{\frac{1}{2}}}. \quad (34)$$

### Geometric and Arithmetic Dependent

- Heuristic G1 (Geometric Dependent 1) is for  $\frac{\eta}{1-\eta} = 1$

$$\mu(\Phi)_{\Psi, \Psi}^{\mathbf{0}, \mathbf{r}}(\mathbf{x}) = \lambda p \xi_{\Psi, \Phi}(\|\mathbf{x}\|)^{\frac{1}{2}} \xi_{\Psi, \Phi}(\|\mathbf{x} - \mathbf{r}\|)^{\frac{1}{2}} \quad (35)$$

and

$$\mu(\Phi)_{\Psi, \Phi}^{\mathbf{0}, \mathbf{r}}(\mathbf{x}) = \lambda p \xi_{\Psi, \Phi}(\|\mathbf{x}\|)^{\frac{1}{2}} \xi_{\Phi, \Phi}(\|\mathbf{x} - \mathbf{r}\|)^{\frac{1}{2}}. \quad (36)$$

- Heuristic  $G_{\rho}$  (Geometric Dependent  $\rho$ ) is for  $\frac{\eta}{1-\eta} = \rho$  with equations given in (21)-(22). Note that a bigger  $\rho$  puts more emphasis on the positive correlation.

- Heuristic A1 (Arithmetic Dependent 1) is for  $\frac{\eta}{1-\eta} = 1$

$$\mu(\Phi)_{\Psi, \Psi}^{\mathbf{0}, \mathbf{r}}(\mathbf{x}) = \lambda p \frac{\xi_{\Psi, \Phi}(\|\mathbf{x}\|) + \xi_{\Psi, \Phi}(\|\mathbf{x} - \mathbf{r}\|)}{2} \quad (37)$$

and

$$\mu(\Phi)_{\Psi, \Phi}^{\mathbf{0}, \mathbf{r}}(\mathbf{x}) = \lambda p \frac{\xi_{\Psi, \Phi}(\|\mathbf{x}\|) + \xi_{\Phi, \Phi}(\|\mathbf{x} - \mathbf{r}\|)}{2}. \quad (38)$$

- Heuristic A $\rho$  (Geometric Dependent  $\rho$ ) is for  $\frac{\eta}{1-\eta} = \rho$  with equations given in (23)-(24). Note that a bigger  $\rho$  puts less emphasis on the positive correlation.

**Combinations** There are dependent version of the latter. For instance

- Heuristic B1G1 corresponds to B1 with independence replaced by GD1, namely:

$$\mu(\Phi)_{\Psi, \Psi}^{\mathbf{0}, \mathbf{r}}(\mathbf{x}) = \lambda p \frac{\xi_{\Psi, \Phi}(\|\mathbf{x}\|)^{\frac{5}{6}} \xi_{\Psi, \Phi}(\|\mathbf{x} - \mathbf{r}\|)^{\frac{2}{3}}}{\xi_{\Psi, \Psi}(r)^{\frac{1}{2}}} \quad (39)$$

and

$$\mu(\Phi)_{\Psi, \Phi}^{\mathbf{0}, \mathbf{r}}(\mathbf{x}) = \lambda p \frac{\xi_{\Psi, \Phi}(\|\mathbf{x}\|)^{\frac{2}{3}} \xi_{\Phi, \Phi}(\|\mathbf{x} - \mathbf{r}\|)^{\frac{1}{2}}}{\xi_{\Psi, \Phi}(r)^{\frac{1}{6}}}. \quad (40)$$

**Mixtures** One can also take mixtures of the above cases. The numbering here is w.r.t. the number of terms in the mixture.

- Heuristic M2BI (Mixture of two types of Bayes Independent) is the following linear combination of BOI and B $\infty$ I:

$$\begin{aligned} \mu(\Phi)_{\Psi, \Psi}^{\mathbf{0}, \mathbf{r}}(\mathbf{x}) &= \frac{\lambda p}{2} \frac{\xi_{\Psi, \Phi}(\|\mathbf{x}\|) \xi_{\Psi, \Phi}(\|\mathbf{x} - \mathbf{r}\|)}{\xi_{\Psi, \Psi}(r)} \\ &+ \frac{\lambda p}{2} \xi_{\Psi, \Phi}(\|\mathbf{x}\|)^{\frac{1}{2}} \xi_{\Psi, \Phi}(\|\mathbf{x} - \mathbf{r}\|)^{\frac{1}{2}} \end{aligned} \quad (41)$$

and

$$\begin{aligned} \mu(\Phi)_{\Psi, \Phi}^{\mathbf{0}, \mathbf{r}}(\mathbf{x}) &= \frac{\lambda p}{2} \xi_{\Psi, \Phi}(\|\mathbf{x}\|) \\ &+ \frac{\lambda p}{2} \frac{\xi_{\Psi, \Phi}(\|\mathbf{x}\|)^{\frac{1}{2}} \xi_{\Phi, \Phi}(\|\mathbf{x} - \mathbf{r}\|)}{\xi_{\Psi, \Phi}(r)^{\frac{1}{2}}}. \end{aligned} \quad (42)$$

- Heuristic M3BI (Mixture of three types of Bayes Independent) is the following linear combination of B0I, B1I and B∞I:

$$\begin{aligned}\mu(\Phi)_{\Psi,\Psi}^{\mathbf{0},\mathbf{r}}(\mathbf{x}) &= \frac{\lambda p \xi_{\Psi,\Phi}(\|\mathbf{x}\|)\xi_{\Psi,\Phi}(\|\mathbf{x}-\mathbf{r}\|)}{3 \xi_{\Psi,\Psi}(r)} \\ &+ \frac{\lambda p \xi_{\Psi,\Phi}(\|\mathbf{x}\|)^{\frac{2}{3}}\xi_{\Psi,\Phi}(\|\mathbf{x}-\mathbf{r}\|)^{\frac{2}{3}}}{3 \xi_{\Psi,\Psi}(r)^{\frac{1}{3}}} \\ &+ \frac{\lambda p \xi_{\Psi,\Phi}(\|\mathbf{x}\|)^{\frac{1}{2}}\xi_{\Psi,\Phi}(\|\mathbf{x}-\mathbf{r}\|)^{\frac{1}{2}}}{3} \quad (43)\end{aligned}$$

and

$$\begin{aligned}\mu(\Phi)_{\Psi,\Phi}^{\mathbf{0},\mathbf{r}}(\mathbf{x}) &= \frac{\lambda p}{3}\xi_{\Psi,\Phi}(\|\mathbf{x}\|) \\ &+ \frac{\lambda p \xi_{\Psi,\Phi}(\|\mathbf{x}\|)^{\frac{2}{3}}\xi_{\Phi,\Phi}(\|\mathbf{x}-\mathbf{r}\|)^{\frac{2}{3}}}{3 \xi_{\Psi,\Phi}(r)^{\frac{1}{3}}} \\ &+ \frac{\lambda p \xi_{\Psi,\Phi}(\|\mathbf{x}\|)^{\frac{1}{2}}\xi_{\Phi,\Phi}(\|\mathbf{x}-\mathbf{r}\|)}{3 \xi_{\Psi,\Phi}(r)^{\frac{1}{2}}}. \quad (44)\end{aligned}$$

- Heuristic M∞BI mixes all Bayes' Independent formulas (there is one for all  $\eta$ ) 'equally': Let  $\eta = (k+l)/(k+2l)$ . By passing to the continuum, one can use (19) and (20) to get the following integral form:

$$\mu(\Phi)_{\Psi,\Psi}^{\mathbf{0},\mathbf{r}}(\mathbf{x}) = \lambda p \int_0^1 \xi_{\Psi,\Phi}(\|\mathbf{x}\|)^\eta \xi_{\Psi,\Phi}(\|\mathbf{x}-\mathbf{r}\|)^\eta \xi_{\Psi,\Psi}(r)^{1-2\eta} d\eta \quad (45)$$

and

$$\mu(\Phi)_{\Psi,\Phi}^{\mathbf{0},\mathbf{r}}(\mathbf{x}) = \lambda p \int_0^1 \xi_{\Psi,\Phi}(\|\mathbf{x}\|)^\eta \xi_{\Phi,\Phi}(\|\mathbf{x}-\mathbf{r}\|)^{2(1-\eta)} \xi_{\Psi,\Phi}(r)^{\eta-1} d\eta. \quad (46)$$

- Heuristic M∞BG1 mixes all Bayes' formulas with geometric mean of parameter 1 'equally', i.e., if  $\eta = (k+l)/(k+2l)$ , then

$$\mu(\Phi)_{\Psi,\Psi}^{\mathbf{0},\mathbf{r}}(\mathbf{x}) = \lambda p \int_0^1 \xi_{\Psi,\Phi}(\|\mathbf{x}\|)^{\frac{1}{2}+\frac{\eta}{2}} \xi_{\Psi,\Phi}(\|\mathbf{x}-\mathbf{r}\|)^{1-\frac{\eta}{2}} \xi_{\Psi,\Psi}(r)^{-\frac{1}{2}} d\eta \quad (47)$$

and

$$\mu(\Phi)_{\Psi,\Phi}^{\mathbf{0},\mathbf{r}}(\mathbf{x}) = \lambda p \int_0^1 \xi_{\Psi,\Phi}(\|\mathbf{x}\|)^{1-\frac{\eta}{2}} \xi_{\Phi,\Phi}(\|\mathbf{x}-\mathbf{r}\|)^{\frac{1}{2}} \xi_{\Psi,\Phi}(r)^{\frac{\eta}{2}-\frac{1}{2}} d\eta. \quad (48)$$

### 5.3 Terminology for Functional and Polynomial Equations

**Integral Equations** When plugging any the above heuristics in Equations (82) and (83) we get a system of integral equations, which will be referred to as the *pairwise-interaction second moment measure functional equations*.

**Polynomial Equations** Each of these functional equations in turn leads to polynomial equations satisfied by the value of the pair correlation functions close to zero. These will be referred to as the *pairwise-interaction second moment measure polynomial equations*. There is a functional and a polynomial equation for each heuristic of the classification. The setting for polynomial equations is as follows: it considers the special case with  $f(r) = \alpha 1_{r < a}$  and (with  $\mu = \lambda \pi a^2$ ), it assumes that  $\mu w > \beta$  and that

- $\xi_{\Psi, \Phi}(\cdot)$  is almost constant on  $(0, a)$  and equal to  $w$ <sup>1</sup>;
- $\xi_{\Phi, \Phi}(\cdot)$  is almost constant on  $(0, a)$  and equal to  $v$ .
- $\xi_{\Psi, \Psi}(\cdot)$  is almost constant on  $(0, a)$  and equal to  $z$ .

For numerical justifications, see Figures 2 and 13 below.

The polynomial equations will be in the three variables  $v, w, z$ . Note that (12) then reads

$$\beta = \alpha \lambda (1 - p) \pi a^2 w = (1 - p) \alpha \mu w. \quad (49)$$

So if there exists a stationary regime, with flat enough pair correlation functions in the said range, then necessarily the variables  $p, v, z$  and  $w$  will satisfy the announced 'polynomial' equation. Note that this is *not* sufficient for the functional equation to have a non-degenerate solution.

**Terminology** Below we use the following code: **f** for functional and **p** for polynomial. For instance f-b1i means the functional equation associated to the B1I heuristic, p-m $\infty$ b1g1 means the polynomial equation of the M $\infty$ B1G1 heuristic, etc.

---

<sup>1</sup>Assuming that  $w < 1$  is equivalent to what we called cluster or second repulsion above; more general assumptions should be considered in the no-motion case

### 5.3.1 Heuristic B1I

**Functional equation** Under Heuristic B1I, the version of (16) is

$$\begin{aligned}
(\beta + \gamma)p\xi_{\Phi, \Phi}(r) &= p\gamma + (1 - p)\xi_{\Psi, \Phi}(r)f(r) \\
&+ \lambda(1 - p)p\xi_{\Psi, \Phi}(r)^{\frac{2}{3}} \int_{\mathbb{R}^2} \xi_{\Psi, \Phi}(\|\mathbf{x}\|)^{\frac{2}{3}} \xi_{\Phi, \Phi}(\|\mathbf{x} - \mathbf{r}\|)^{\frac{2}{3}} f(\|\mathbf{x}\|) d\mathbf{x} \\
\beta p\xi_{\Psi, \Phi}(r) &= (1 - p)\gamma(\xi_{\Psi, \Psi}(r) - 1) \\
&+ \lambda(1 - p)p\xi_{\Psi, \Psi}(r)^{\frac{2}{3}} \int_{\mathbb{R}^2} \xi_{\Psi, \Phi}(\|\mathbf{x}\|)^{\frac{2}{3}} \xi_{\Phi, \Phi}(\|\mathbf{x} - \mathbf{r}\|)^{\frac{2}{3}} f(\|\mathbf{x}\|) d\mathbf{x}.
\end{aligned} \tag{50}$$

**Polynomial equation** The associated polynomial equations read

$$\begin{aligned}
(\gamma + \beta)pv &= \gamma p + \alpha(1 - p)w + \beta pv^{\frac{2}{3}}w^{\frac{1}{3}} \\
\beta pw &= (1 - p)\gamma(z - 1) + \beta pz^{\frac{2}{3}}w^{\frac{1}{3}} \\
\beta &= (1 - p)\alpha\mu w \\
1 &= (1 - p)^2z + 2p(1 - p)w + p^2v.
\end{aligned} \tag{51}$$

### 5.3.2 Heuristic B1G1

**Functional equation** Under Heuristic B1G1, the version of (16) is

$$\begin{aligned}
(\beta + \gamma)p\xi_{\Phi, \Phi}(r) &= p\gamma + (1 - p)\xi_{\Psi, \Phi}(r)f(r) \\
&+ \lambda(1 - p)p\xi_{\Psi, \Phi}(r)^{\frac{5}{6}} \int_{\mathbb{R}^2} \xi_{\Psi, \Phi}(\|\mathbf{x}\|)^{\frac{5}{6}} \xi_{\Phi, \Phi}(\|\mathbf{x} - \mathbf{r}\|)^{\frac{1}{2}} f(\|\mathbf{x}\|) d\mathbf{x} \\
\beta p\xi_{\Psi, \Phi}(r) &= (1 - p)\gamma(\xi_{\Psi, \Psi}(r) - 1) \\
&+ \lambda(1 - p)p\xi_{\Psi, \Psi}(r)^{\frac{1}{2}} \int_{\mathbb{R}^2} \xi_{\Psi, \Phi}(\|\mathbf{x}\|)^{\frac{5}{6}} \xi_{\Phi, \Phi}(\|\mathbf{x} - \mathbf{r}\|)^{\frac{2}{3}} f(\|\mathbf{x}\|) d\mathbf{x}.
\end{aligned} \tag{52}$$

**Polynomial equation** The associated polynomial equations read

$$\begin{aligned}
(\gamma + \beta)pv &= \gamma p + \alpha(1 - p)w + \beta pv^{\frac{1}{2}}w^{\frac{1}{2}} \\
\beta pw &= (1 - p)\gamma(z - 1) + \beta pz^{\frac{1}{2}}w^{\frac{1}{2}} \\
\beta &= (1 - p)\alpha\mu w \\
1 &= (1 - p)^2z + 2p(1 - p)w + p^2v.
\end{aligned} \tag{53}$$

### 5.3.3 Heuristic M2BI

**Functional equation** Under Heuristic M2BI, the version of (16) is

$$\begin{aligned}
(\beta + \gamma)p\xi_{\Phi, \Phi}(r) &= p\gamma + (1-p)\xi_{\Psi, \Phi}(r)f(r) \\
&+ \frac{1}{2}\lambda(1-p)p\xi_{\Psi, \Phi}(r) \int_{\mathbb{R}^2} \xi_{\Psi, \Phi}(\|\mathbf{x}\|)f(\|\mathbf{x}\|)d\mathbf{x} \\
&+ \frac{1}{2}\lambda(1-p)p\xi_{\Psi, \Phi}(r)^{\frac{1}{2}} \int_{\mathbb{R}^2} \xi_{\Psi, \Phi}(\|\mathbf{x}\|)^{\frac{1}{2}}\xi_{\Phi, \Phi}(\|\mathbf{x} - \mathbf{r}\|)f(\|\mathbf{x}\|)d\mathbf{x} \\
\beta p\xi_{\Psi, \Phi}(r) &= (1-p)\gamma(\xi_{\Psi, \Psi}(r) - 1) \\
&+ \frac{1}{2}\lambda(1-p)p \int_{\mathbb{R}^2} \xi_{\Psi, \Phi}(\|\mathbf{x}\|)\xi_{\Psi, \Phi}(\|\mathbf{x} - \mathbf{r}\|)f(\|\mathbf{x}\|)d\mathbf{x}. \\
&+ \frac{1}{2}\lambda(1-p)p\xi_{\Psi, \Psi}(r) \int_{\mathbb{R}^2} \xi_{\Psi, \Phi}(\|\mathbf{x}\|)^{\frac{1}{2}}\xi_{\Psi, \Phi}(\|\mathbf{x} - \mathbf{r}\|)^{\frac{1}{2}}f(\|\mathbf{x}\|)d\mathbf{x}.
\end{aligned} \tag{54}$$

This should again be complemented by

$$p = 1 - \frac{\beta}{\lambda 2\pi \int_{\mathbb{R}^+} \xi_{\Psi, \Phi}(r)f(r)rdr}, \tag{55}$$

and

$$\xi_{\Psi, \Psi}(r) = \frac{1}{(1-p)^2} \left( 1 - (p)^2 \xi_{\Phi, \Phi}(r) - 2p(1-p) \xi_{\Psi, \Phi}(r) \right). \tag{56}$$

**Polynomial equation** The associated polynomial equations read

$$\begin{aligned}
(2\gamma + \beta)pv &= 2\gamma p + 2\alpha(1-p)w + \beta pw \\
\beta pw &= (1-p)\gamma(z-1) + \frac{1}{2}\beta pw + \frac{1}{2}\beta pz \\
\beta &= (1-p)\alpha\mu w \\
1 &= (1-p)^2 z + 2p(1-p)w + p^2 v.
\end{aligned} \tag{57}$$

Using the last and the second equations, we can eliminate  $z$  to get

$$\beta p(1-p)^2 w = (1-2p(1-p)w - p^2 v)(2\gamma(1-p) + \beta p) - 2\gamma(1-p)^3. \tag{58}$$

This in turn gives

$$\begin{aligned}
(2\gamma + \beta)v(\alpha\mu w - \beta) &= 2\gamma(\alpha\mu w - \beta) + 2\alpha\beta w + \beta w(\alpha\mu w - \beta) \\
w(\alpha\mu w - \beta)\beta^2 &= -2\gamma\beta^2 \\
&+ (\alpha\mu w - \beta + 2\gamma)(w^2\alpha^2\mu^2 - (\alpha\mu w - \beta)^2 v - 2\beta(\alpha\mu w - \beta)w).
\end{aligned}$$



When now eliminating  $v$  in the last system, we get that  $w$  satisfies the degree 4 equation:

$$\begin{aligned} & (2\gamma + \beta)((\alpha\mu w - \beta + 2\gamma)(w^2\alpha^2\mu^2 - 2\beta(\alpha\mu w - \beta)w) + w(\alpha\mu w - \beta)\beta^2 - 2\gamma\beta^2) \\ &= (\alpha\mu w - \beta)(\alpha\mu w - \beta + 2\gamma)(2\gamma(\alpha\mu w - \beta) + 2\alpha\beta w + \beta w(\alpha\mu w - \beta)). \end{aligned} \quad (59)$$

### 5.3.4 Heuristic $M_{\infty}BI$

**Functional equation** Under Heuristic  $M_{\infty}BI$ , the version of (16) is

$$\begin{aligned} & (\beta + \gamma)p\xi_{\Phi,\Phi}(r) = p\gamma + (1 - p)\xi_{\Psi,\Phi}(r)f(r) \\ & + \lambda(1 - p)p \int_{\mathbb{R}^2} \int_0^1 \xi_{\Psi,\Phi}(\|x\|)^{\eta} \xi_{\Phi,\Phi}(\|x - (r, 0)\|)^{2(1-\eta)} \xi_{\Psi,\Phi}(r)^{\eta} f(\|x\|) d\eta dx \\ & \beta p \xi_{\Psi,\Phi}(r) = (1 - p)\gamma (\xi_{\Psi,\Psi}(r) - 1) \\ & + \lambda(1 - p)p \xi_{\Psi,\Psi}(r) \int_{\mathbb{R}^2} \int_0^1 \xi_{\Psi,\Phi}(\|x\|)^{\eta} \xi_{\Psi,\Phi}(\|x - (r, 0)\|)^{\eta} f(\|x\|) \xi_{\Psi,\Psi}(r)^{1-2\eta} d\eta dx. \end{aligned} \quad (60)$$

This should again be complemented by (55) and (56).

**Polynomial equation** The associated polynomial<sup>2</sup> equations read

$$\begin{aligned} (\gamma + \beta)pv &= \gamma p + \alpha(1 - p)w + \beta p \frac{1}{w} \frac{v^2 - w^2}{\log(v^2) - \log(w^2)} \\ \beta pw &= (1 - p)\gamma(z - 1) + \beta p \frac{1}{w} \frac{w^2 - z^2}{\log(w^2) - \log(z^2)} \\ \beta &= (1 - p)\alpha\mu w \\ 1 &= (1 - p)^2 z + 2p(1 - p)w + p^2 v. \end{aligned} \quad (61)$$

This should again be complemented by (55) and (56).

---

<sup>2</sup>This is an abuse of terminology here

### 5.3.5 Heuristic $M_{\infty}BG1$

**Functional equation** Under Heuristic  $M_{\infty}BG1$ , the version of (16) is

$$\begin{aligned}
(\beta + \gamma)p\xi_{\Phi, \Phi}(r) &= p\gamma + (1 - p)\xi_{\Psi, \Phi}(r)f(r) \\
+\lambda(1 - p)p\xi_{\Psi, \Phi}(r) \int_{\mathbb{R}^2} \int_0^1 &\xi_{\Psi, \Phi}(\|x\|)^{1-\frac{\eta}{2}}\xi_{\Phi, \Phi}(\|x - (r, 0)\|)^{\frac{1}{2}}\xi_{\Psi, \Phi}(r)^{\frac{\eta}{2}-\frac{1}{2}}f(\|x\|)d\eta dx \\
\beta p\xi_{\Psi, \Phi}(r) &= (1 - p)\gamma(\xi_{\Psi, \Psi}(r) - 1) \\
+\lambda(1 - p)p\xi_{\Psi, \Psi}(r) \int_{\mathbb{R}^2} \int_0^1 &\xi_{\Psi, \Phi}(\|x\|)^{\frac{1}{2}+\frac{\eta}{2}}\xi_{\Psi, \Phi}(\|x - (r, 0)\|)^{1-\frac{\eta}{2}}f(\|x\|)\xi_{\Psi, \Psi}(r)^{-\frac{1}{2}}d\eta dx.
\end{aligned} \tag{62}$$

This should again be complemented by (55) and (56).

**Polynomial equation** The associated polynomial equations read

$$\begin{aligned}
(\gamma + \beta)pv &= \gamma p + \alpha(1 - p)w + \beta pv^{\frac{1}{2}}w^{\frac{1}{2}} \\
\beta pw &= (1 - p)\gamma(z - 1) + \beta pz^{\frac{1}{2}}w^{\frac{1}{2}} \\
\beta &= (1 - p)\alpha\mu w \\
1 &= (1 - p)^2z + 2p(1 - p)w + p^2v.
\end{aligned} \tag{63}$$

So  $p\text{-b1g1}$  and  $p\text{-m}\infty\text{bg1}$  are the same.

## 5.4 Numerical Results

In this section, we compare the fraction of infected nodes as obtained by our integral and polynomial systems and discrete event simulation. For the latter, the system evolves on a square with edges wrapped around to form a torus so as to avoid border effects. Points move according to the mobility model defined above. The shot-noise or infection function is  $f(r) = \alpha 1_{r \leq a}$ .

Tables 1, 2 and 3 study the effect of mobility for a variety of Boolean-percolation and recovery rate scenarios.

Instances of pair correlation functions obtained from the functional equation numerical scheme associated with Heuristic  $f\text{-mb2}$  are given in Figure 2. All numerical solutions of integral equations lead to similar pictures, which justifies the polynomial heuristics.

## 5.5 A Tentative Phase Diagram

The polynomial systems described above lead to a phase diagram. The simplest description of the latter is the  $(\mu, \gamma)$ -phase diagram, which is predicted by the mono-

$\gamma$	0	.2	1	5	$\infty$
$p_{\text{sim}}$	0.26	0.28	0.29	0.33	0.36
$p_{\text{p-b1i}}$	0.313	0.315	0.323	0.341	0.363
$p_{\text{p-b1g1}}$	0.325	0.326	0.331	0.343	0.363
$p_{\text{p-m2bi}}$	0.328	0.328	0.329	0.341	0.363
$p_{\text{p-m}\infty\text{bi}}$	0.33	0.33	0.33	0.34	0.36
$p_{\text{f-h0}}$	0.23	0.28	0.29	0.32	0.36
$p_{\text{p-h0}}$	0.23	0.25	0.27	0.32	0.36

Table 1: Effect of mobility. Way above Boolean-percolation. Fraction of infected nodes ( $p$ ) obtained by simulation, the functional fixed point equation and the polynomial equation. This is for  $\beta = 8$ ,  $a = 2$ ,  $\lambda = 1$  and  $\alpha = 1$ , so that  $\mu \sim 12.56$ . The agreement with simulation is good. Both b1 and m2bi slightly overestimate  $p$ , with b1i being here a bit closer than the others.

$\gamma$	0+	0.1	1	10	$\infty$
$p_{\text{sim}}$			0.22	0.31	0.36
$p_{\text{p-b1i}}$	0.176	0.188	0.253	0.342	0.363
$p_{\text{p-b1g1}}$	0.205	0.213	0.264	0.348	0.363
$p_{\text{p-m2bi}}$	0.245	0.240	0.254	0.336	0.363
$p_{\text{p-m}\infty\text{bi}}$	0.26	0.26	0.27	0.34	0.36

Table 2: Effect of mobility. Below percolation, medium recovery rate. Fraction of infected nodes ( $p$ ) obtained by simulation, the functional fixed point equation and the polynomial equation. This is for  $\beta = 2$ ,  $a = 1$ ,  $\lambda = 1$  and  $\alpha = 1$ , so that  $\mu \sim 3.14$ . Simulation is inefficient at low speeds. The agreement with simulation is again good when available. Both b1 and m2bi slightly overestimate  $p$  and provide similar results.

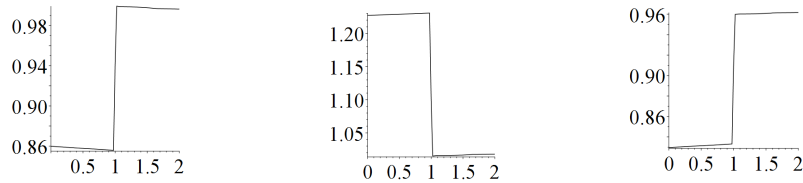


Figure 2: Left: the  $\xi_{\Psi, \Phi}(r)$  function; Center: the  $\xi_{\Phi, \Phi}(r)$  function; Right: the  $\xi_{\Psi, \Psi}(r)$  function. Here,  $\beta = 1$ ,  $a = 1$ ,  $\lambda = 1$ ,  $\gamma = 1$ , and  $\alpha = 1$ .

$\gamma$	0+	0.01	0.1	.2	1	5	100
$p_{\text{sim}}$				0.54	0.61	0.66	0.68
$p_{\text{p-b1i}}$	0.478		0.503	0.523	0.599	0.657	0.680
$p_{\text{p-b1g1}}$	0.530		0.544	0.557	0.609	0.658	0.680
$p_{\text{p-m2bi}}$	0.523		0.538	0.551	0.605	0.656	0.680
$p_{\text{p-m}\infty\text{bi}}$		0.54	0.55	0.56	0.61	0.66	0.68

Table 3: Effect of mobility. Below Boolean-percolation, low recovery rate. Fraction of infected nodes ( $p$ ) obtained by simulation, the functional fixed point equation and the polynomial equation. This is for  $\beta = 1$ ,  $a = 1$ ,  $\lambda = 1$  and  $\alpha = 1$ , so that  $\mu \sim 3.14$ . The agreement with simulation is again good when available and again provide similar results.

tonicity properties of the SIS dynamics: there exists a function  $\beta_c = \beta_c(\alpha, \mu, \gamma)$ , which will be referred to as the *extinction-survival critical recovery rate* such that there is survival for all  $\beta < \beta_c$  and extinction above.

The main novelty here is the  $(\mu, \beta)$ -phase diagram. When fixing  $\alpha$ , this diagram consists in a partition of the  $(\mu, \beta)$  positive orthant in 3 disjoint regions:

- A *safe region* where the epidemic is always extinct regardless of the positive motion rate. This region is the wedge  $\beta > \alpha\mu$ .
- An *unsafe region* which is the geometric complement of the latter; in this region, there are motion rates such that the epidemic survives.

The unsafe region can in turn be partitioned into a *motion-insensitive* (UMI) and a *motion-sensitive* (UMS) region:

- In the UMI region, the epidemic *always survives*, regardless of the positive motion rate. This region is wedge-like too, of the form  $\mu > \mu_0$ ,  $\beta < \beta_0(\mu)$ . Here  $\mu_0$  is an absolute constant smaller than the percolation threshold  $\mu_*$ , and  $\beta_0(\cdot)$  is a function to be specified, which will be referred to as the *motion-sensitivity critical recovery rate*.
  - In the part of the UMI region where  $\mu < \mu_*$ , the epidemic is extinct for 0 motion and survives for all non-zero motion rates.
  - In the part of the UMI region where  $\mu > \mu_*$ , the epidemic survives for all motion rates, including 0 motion.
- In the UMS region, the epidemic survives if motion is *low or high enough*. More precisely there exist functions  $\gamma_c^+(\alpha, \mu, \beta)$  (the upper extinction-survival

critical motion rate) and  $\gamma_c^-(\alpha, \mu, \beta)$  (the lower extinction-survival critical motion rate), to be specified, such that there is survival if  $\gamma < \gamma_c^-$  or  $\gamma > \gamma_c^+$ , and extinction otherwise. This region is a strip-like region of the form  $\beta_0(\mu) < \beta < \alpha\mu$ , with  $\beta_0(\mu) = 0$  when  $\mu < \mu_0$ .

- In the part of the UMS region where  $\mu < \mu_*$ , the epidemic is extinct for 0 motion, survives for small enough motion rates, is extinct for intermediate motion rates, and survives for high enough motion rates.
- In the part of the UMS region above  $\mu_*$ , the epidemic survives for no and small enough motion rate, is extinct for intermediate motion rates, and survives for high enough motion rates.

This phase diagram is depicted in Figure 1.

This phase diagram is obtained when studying certain singularities of the polynomial systems. The exact values of the constants and functions introduced in the phase diagram depend on the heuristic, but the global picture is the same for all in spite of numerical discrepancies. The picture that emerges from this analysis is consistent for all heuristics and partially substantiated by simulation. We first proceed with the analysis of the singularities of the polynomial systems and then discuss the simulation validation.

## 5.6 Critical Values

From the structural results, we know that for all  $\gamma > 0$ , there is a critical value of  $\beta$ ,  $\beta_c = \beta_c(\gamma)$ , *strictly less than*  $\alpha\mu$ , such that the epidemics is extinct if  $\beta > \beta_c$  and survives if  $\beta < \beta_c$ .

There is no proof of existence of a critical value  $\gamma_c$  above which survival holds and below which there is no survival. In fact the analysis of the present paper suggests that this is not the case at all. However, when decreasing  $\gamma$  from  $\infty$  (where the epidemic survives if  $\mu\alpha > \beta$ ), if we are below Boolean percolation, there ought to be a  $\gamma_c^+$  which is the largest  $\gamma$  such that above this value the epidemic survives but not immediately below.

Let us now see what the polynomial heuristics say on the matter.

### 5.6.1 M2BI

A direct analysis of the roots of (57) around  $p \sim 0$  gives that  $p \sim 0$  is only possible if

$$8(\mu\alpha - \beta)\gamma^2 + 2\beta(3(\mu\alpha - \beta) - 2\alpha)\gamma + \beta^2(\mu\alpha - \beta) = 0. \quad (64)$$

This is easily obtained when showing that the first equation in (57) implies that

$$v(p)p \xrightarrow{p \rightarrow 0} \frac{2\beta}{\mu(2\gamma + \beta)}$$

and by using this fact in (58) when making an expansion in  $p$  close to 0.

When looking at (64) as a quadratic in  $\gamma$ , we get that if there exists a positive (resp. negative) solution, then the other solution is positive (resp. negative). For real solutions to exist, it is necessary and sufficient to have either

$$\mu\alpha - \beta \leq \frac{2\alpha}{3 + \sqrt{8}} \sim \alpha 0.343 \quad (65)$$

or

$$\mu\alpha - \beta \geq \frac{2\alpha}{3 - \sqrt{8}} \sim \alpha 11.65. \quad (66)$$

This is easily obtained when studying the discriminant of (64). If these inequalities are not satisfied, then this discriminant is negative, so that there is no real valued  $\gamma$  solving (64). If (65) holds, then there are two positive roots. If (66) holds, then there are two negative roots, which for us is equivalent to no root.

Below, we focus on the region (65), which is the only one in which criticality is possible. Let

$$\mu_0 = \alpha\eta := \alpha \frac{2}{3 + \sqrt{8}}. \quad (67)$$

If  $\mu < \mu_0$ , then (65) holds so that there exist two positive  $\gamma$  solving (64), say  $0 < \gamma_c^- < \gamma_c^+$ .

If  $\mu > \mu_0$ , then there exists a  $\beta_0(\mu, \alpha)$  defined by

$$\beta_0 = \mu\alpha - \eta\alpha, \quad (68)$$

such that if  $\beta < \beta_0$ , then the quadratic equation (64) has no real root in  $\gamma$ , which means that any positive motion results in survival,<sup>3</sup> whereas if  $\beta > \beta_0$ , then the roots  $0 < \gamma_c^- < \gamma_c^+$  exist. The upper phase transition w.r.t.  $\gamma$  takes place at  $\gamma_c^+$ : Above  $\gamma_c^+$ , there is survival, and below  $\gamma_c^+$ , there is extinction. Indeed, we conjecture that the system has a positive fraction of infected nodes for infinite  $\gamma$ , and the threshold of interest is hence that obtained when decreasing  $\gamma$  from infinity and looking at the largest  $\gamma$  above which the epidemic survives. We have

$$\gamma_c^+(\alpha, \mu, \beta) = \beta \frac{2\alpha - 3(\mu\alpha - \beta) + \sqrt{(2\alpha - 3(\mu\alpha - \beta))^2 - 8(\mu\alpha - \beta)^2}}{8(\mu\alpha - \beta)} \quad (69)$$

---

<sup>3</sup> note that this is consistent with what we see in Tables 2 and 3, where the discrepancy between  $\mu$  and  $\beta/\alpha$  is above 0.343 and where the epidemics seems to persist for all  $\gamma > 0$ .

and

$$\gamma_c^-(\alpha, \mu, \beta) = \beta \frac{2\alpha - 3(\mu\alpha - \beta) - \sqrt{(2\alpha - 3(\mu\alpha - \beta))^2 - 8(\mu\alpha - \beta)^2}}{8(\mu\alpha - \beta)}. \quad (70)$$

Since there is survival for  $\gamma > \gamma_c^+$ , it ought to be that for  $\gamma \in (\gamma_c^-, \gamma_c^+)$ , there is extinction. By the same argument, for  $\gamma < \gamma_c^-$ , there is survival.

Note that if  $\beta = \beta_0$ , then the corresponding value of  $\gamma_c^+ = \gamma_c^-$  is

$$\gamma_0(\alpha, \mu) = \frac{\beta_0(2\alpha - 3(\mu\alpha - \beta_0))}{8(\mu\alpha - \beta_0)} = \frac{(\mu\alpha - \eta\alpha)(2\alpha - 3\eta\alpha)}{8\eta\alpha} = \frac{\alpha(\mu - \eta)(2 - 3\eta)}{8\eta}. \quad (71)$$

The last function is just an affine function in  $\mu$  with positive slope. It is strictly positive for  $\mu > \mu_0 \sim 0.343$ .

Hence we get the following m2bi  $(\mu, \beta)$ -phase diagram:

**Result 4.** Assume that  $\mu\alpha > \beta$ .

- In the motion-subcritical regions, namely for all  $\mu < \mu_0$ , with  $\mu_0$  given by (67), the system is motion-sensitive and there is survival for all values of  $\gamma$  larger  $\gamma_c^+$  or smaller than  $\gamma_c^-$ , and extinction for  $\gamma$  between these two values, with  $\gamma_c^+$  and  $\gamma_c^-$  given by (69) and (70) respectively.
- In the motion-supercritical region, namely for all  $\mu > \mu_0$ ,
  - if  $\beta < \beta_0$ , with  $\beta_0$  defined in (68), the system is motion-insensitive in that there is survival for all positive values of  $\gamma$ ;
  - if  $\beta > \beta_0$ , then the system is motion sensitive.

Instances of the functions  $\beta \rightarrow \gamma_c^+(\beta)$  and  $\beta \rightarrow \gamma_c^-(\beta)$  are depicted in Figure 3.

One can also use the same method to analyze the critical function  $\beta_c$ . There are two ways of evaluating this quantity.

The first one is obtained from (64). The  $\beta_c$  function satisfies the following polynomial equation of degree 3 in  $\beta$ :

$$\beta^3 + \beta^2(6\gamma - \alpha\mu) + \beta 2\gamma(2\alpha - 3\mu\alpha + 4\gamma) - 8\mu\alpha\gamma^2 = 0. \quad (72)$$

There is numerical evidence that this degree three equation has a single positive root that will be denoted  $\beta_c(\alpha, \mu, \gamma)$ .

The second approach consists in devising the local "inverse" of the  $\beta \rightarrow \gamma_c(\beta)$  function discussed above. As illustrated by the left part of Figure 3 for  $\gamma$  small, the inverse function  $\gamma \rightarrow \beta_c(\gamma)$  should be decreasing. It should then reach a minimum at  $\gamma = \gamma_0$  and then increase to  $\mu\alpha$  for  $\gamma$  large. This is in line with what we see on Fig. 4. Hence we get the following p-m2bi  $(\mu, \gamma)$ -phase diagram:

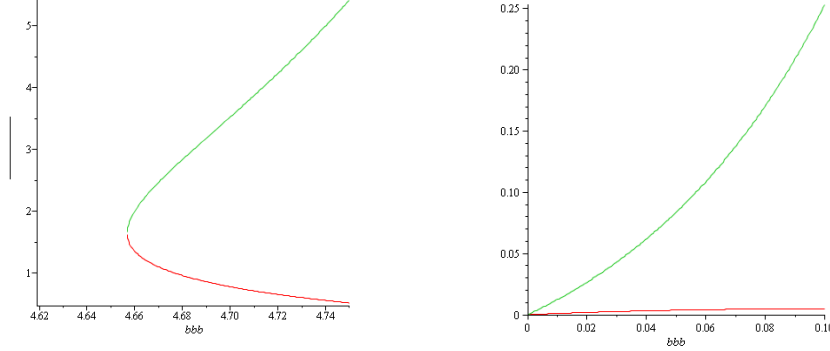


Figure 3: The p-m2bi  $\gamma_c^+$  (green) and  $\gamma_c^-$  (red) functions. The  $x$ -axis represents  $\beta$ . Left:  $\alpha = 1$  and  $\mu = 5 > \mu_0$ ; there is survival on the left of the curve and extinction on the right. If  $\beta < \beta_0$ , where  $\beta_0$  is the largest  $c$  such that the line  $\beta = c$  does not intersect the  $\gamma_c$  curves, the epidemic is motion-insensitive. Right:  $\alpha = 1$  and  $\mu = .25 < \mu_0$ ; there is survival above the green curve and below the red one. There is extinction between the two curves. There is no positive  $\beta$  making the epidemic motion-insensitive. Notice that the  $\gamma_c^-$  function is increasing for small  $\beta$ . It reaches a maximum and then decreases to 0 when  $\beta$  is large.

**Result 5.** *There is survival for all  $\beta < \beta_c$  and extinction above with  $\beta_c = \beta_c(\alpha, \mu, \gamma)$  solution of (72).*

- *If  $\mu < \mu_0$ , then the function  $\gamma \rightarrow \beta_c(\alpha, \mu, \gamma)$  is discontinuous.*
- *If  $\mu > \mu_0$ , then the function  $\gamma \rightarrow \beta_c(\alpha, \mu, \gamma)$  is continuous.*

Instances of the function  $\gamma \rightarrow \beta_c(\gamma)$  defined through (72) are plotted in Figure 4 where we see that it is *not monotonic* in  $\gamma$  in general.

### 5.6.2 BII

By an analysis of the polynomial system similar to that for m2bi above, we get that  $p \sim 0$  is only possible if

$$2(\mu\alpha - \beta)\gamma^2 + (2\beta(\mu\alpha - \beta) + \beta^2(\rho - 1) - \beta\alpha)\gamma + \beta^3(\rho - 1) = 0, \quad (73)$$



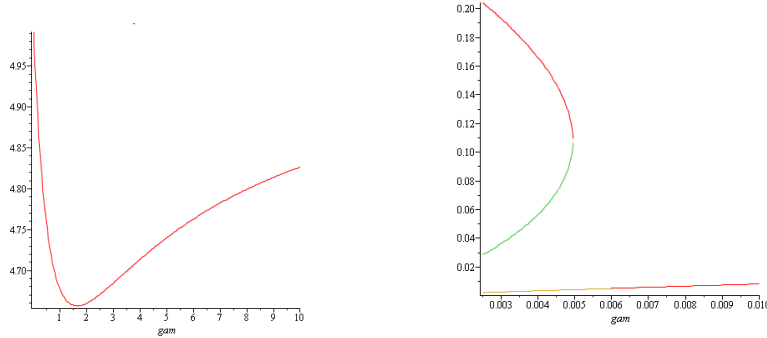


Figure 4: The p-m2bi  $\beta_c(\gamma)$  function for  $\alpha = 1$ . On the  $x$  axis, the variable is  $\gamma$ . Left:  $\mu = 5$ ; there is extinction above the curve and survival below. Right:  $\mu = .25$ . The three roots are jointly represented. The interpretation of  $\beta_c$  as the pseudo-inverse of  $\gamma_c$  suggests that the  $\beta_c$  function should be the upper envelope of these curves (this upper envelope is not depicted). To see this, use the fact that the function  $\gamma_c^-$  is non monotonic in this case. The discontinuity is at the point where  $\gamma_c^-$  reaches its maximum.

with  $\rho = \left(\frac{\alpha\mu}{\beta}\right)^{\frac{2}{3}} > 1$ . By looking at the discriminant of this quadratic, we get that a necessary (but not sufficient) condition for a positive real root to exist is that

$$\mu\alpha < \beta + 1 + \frac{\alpha}{2}.$$

In words,  $\mu\alpha$  has to be close enough to  $\beta$ .

Here is a more precise analysis. There are two real roots (which are necessarily both positive) iff

$$\Delta := (2\beta(\mu\alpha - \beta) + \beta^2(\rho - 1) - \beta\alpha)^2 - 8(\mu\alpha - \beta)\beta^3(\rho - 1) > 0$$

and in this case,

$$\gamma_c^+(\alpha, \mu, \beta) = \frac{\beta(\alpha - 2(\mu\alpha - \beta)) - \beta^2(\rho - 1) + \sqrt{\Delta}}{4(\mu\alpha - \beta)} \quad (74)$$

and

$$\gamma_c^-(\alpha, \mu, \beta) = \frac{\beta(\alpha - 2(\mu\alpha - \beta)) - \beta^2(\rho - 1) - \sqrt{\Delta}}{4(\mu\alpha - \beta)}. \quad (75)$$

These two roots are plotted in Fig. 5.

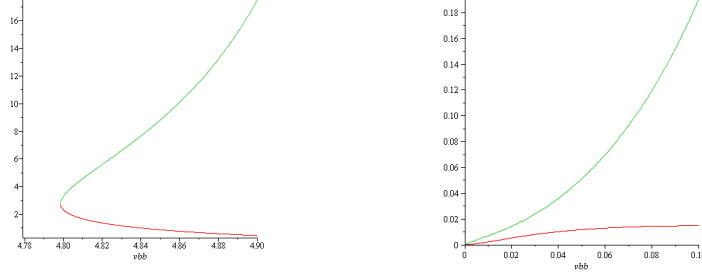


Figure 5: The p-bli functions  $\gamma_c^+(\beta)$  (in green) and  $\gamma_c^-(\beta)$  (in red) for  $\alpha = 1$ . Left:  $\mu = 5$ . Right:  $\mu = .25$ .

For  $\gamma > \gamma_c^+$  (in particular for  $\gamma$  very large), there is survival. For  $\gamma_c^- < \gamma < \gamma_c^+$ , there is extinction, and when  $0 < \gamma < \gamma_c^-$ , there is survival again. We will give an interpretation of these phenomena below.

To be proved: there exists a  $\mu_0$  (for  $\alpha = 1$ ,  $\mu_0 \sim 0.263$  - for p-b1g1 0.306) such that (i) for  $\mu < \mu_0$ , and all  $\beta < \alpha\mu$ ,  $\Delta > 0$  and hence  $\gamma_c^+$  and  $\gamma_c^-$  exist, and (ii) for all values of  $\mu > \mu_0$ , there a minimal  $\beta$ , say  $\beta_0 = \beta_0(\alpha\mu)$ , for  $\Delta$  to be positive and hence for non-degenerate  $\gamma_c^+$  and  $\gamma_c^-$  to exist. In the latter case, the function  $\alpha\mu \rightarrow \beta_0(\alpha\mu)$  is solution of

$$(2\beta(\mu\alpha - \beta) + \beta^2(\rho - 1) - \beta\alpha)^2 = 8(\mu\alpha - \beta)\beta^3(\rho - 1). \quad (76)$$

The  $\beta_0$  function is plotted in Figure 6. At  $\beta_0$ ,  $\gamma_c^+ = \gamma_c^- := \gamma_0$ , with  $\gamma_0$  strictly

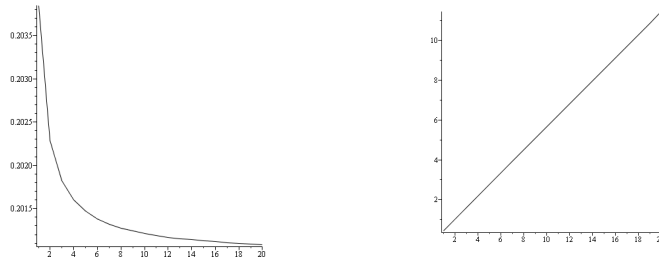


Figure 6: Left: The p-bli function  $\mu - \beta_0(\mu)$  for  $\alpha = 1$ . Right: The p-bli function  $\gamma_0(\mu)$  for  $\alpha = 1$ .

positive. The function  $\gamma_0$  is  $\gamma_c$  for  $\beta = \beta_0$ . It is plotted in Figure 6.

We summarize this in the following p-bli  $(\mu, \beta)$ -phase diagram:

**Result 6.** Assume that  $\mu\alpha > \beta$ .

- In the motion-subcritical region  $\mu < \mu_0$ , the discriminant is positive and there is survival for values of  $\gamma$  larger than  $\gamma_c^+(\alpha\mu, \beta)$  given by (74) or smaller than  $\gamma_c^-$  (75) and extinction for  $\gamma$  between these two values.
- In the motion-supercritical region  $\mu > \mu_0$ ,
  - If  $\beta < \beta_0(\alpha\mu)$ , with  $\beta_0$  solution of (76), we have motion-insensitivity;
  - If  $\beta > \beta_0(\alpha\mu)$ , then there motion sensitivity as above.

Consider now the function  $\gamma \rightarrow \beta_c(\gamma)$  function. Locally, this is just the inverse (in the sense of increasing functions) of the last function. It can also be obtained as a solution of (73). More precisely, we have the following p-bli  $(\mu, \gamma)$ -phase diagram:

**Result 7.** There is survival for all  $\beta < \beta_c$  and extinction above with  $\beta_c = \beta_c(\alpha, \mu, \gamma)$  solution of (73) which can be seen as a degree 9 polynomial in  $\beta$ .

This function is depicted in Figure 7.

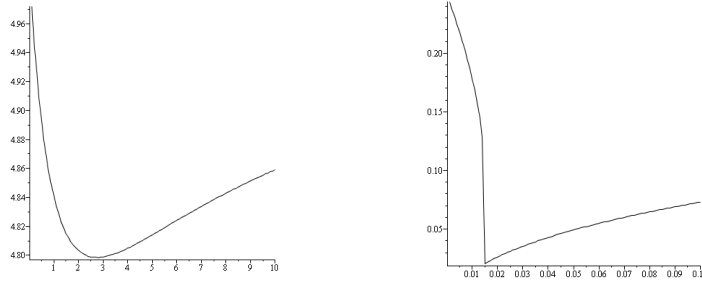


Figure 7: The p-bli function  $\beta_c(\gamma)$ . Left:  $\alpha\mu = 5$ . Right:  $\alpha\mu = .25$ .

## 5.7 Simulation Validation

### 5.7.1 Stationary densities

This subsection gives simulation based fractions of infected nodes in various regions of the phase diagram and compares them to the polynomial solutions.

**Motion-insensitive, Boolean subcritical example** In this region, *any positive motion* instantly transforms the epidemic from extinct to surviving. This is illustrated by the results of Tables 4 and 5 (where simulation and second order heuristics convene).

$\gamma$	.1	.5	1	2	5	10	100	$\infty$
$p_{\text{sim}}$	0.04	0.14	0.20	0.23	0.28			
$p_{\text{p-b1g1}}$	0.18	0.21	0.23	0.26	0.29	0.31	0.33	0.33
$p_{\text{p-m2bi}}$	0.21	0.21	0.22	0.25	0.28	0.30	0.33	0.33

Table 4: Effect of mobility. Boolean-subcritical ( $\mu = 3$ ), motion-supercritical ( $\mu > \mu_0$ ), motion-insensitive ( $\beta < \beta_0$ ) case. Fraction of infected nodes ( $p$ ) obtained by simulation, the functional fixed point equation and the polynomial equation. This is for  $\beta = 2$ ,  $a = 1$ ,  $\lambda \sim 0.955$  and  $\alpha = 1$ , so that  $\mu = 3$ . According to p-b1i, p-b1g1, and p-m2bi, the threshold  $\gamma_c$  is equal to 0. This means that the epidemic survives for all positive speeds  $\gamma$ , in spite of the fact that it dies out for  $\gamma = 0$ .

$\gamma$	.1	.5	1	2	5	10	100	$\infty$
$p_{\text{sim}}$	.09		0.47			0.59		
$p_{\text{p-b1g1}}$	0.18	0.36	0.45	0.52	0.57	0.58	0.60	0.60
$p_{\text{p-m2bi}}$	0.21	0.37	0.45	0.52	0.56	0.58	0.60	0.60

Table 5: Effect of mobility, way below Boolean-percolation. Boolean-subcritical ( $\mu = 1$ ), motion-supercritical ( $\mu > \mu_0$ ), motion-insensitive ( $\beta < \beta_0$ ) case. Fraction of infected nodes ( $p$ ) obtained by simulation, the functional fixed point equation and the polynomial equation. This is for  $\beta = 0.4$ . According to p-b1i, p-b1g1, and p-m2bi,  $\gamma_c = 0$ . The epidemic survives for all positive speeds  $\gamma$ , in spite of the fact that it dies for  $\gamma = 0$ .

**Motion-sensitive and Boolean-subcritical example** In this region, for  $\gamma$  equal to 0, the epidemic dies out; for positive but small values of  $\gamma$  (more precisely, for  $0 < \gamma < \gamma_c^-$  with  $\gamma_c^- > 0$ ), the epidemic survives; for intermediate values of  $\gamma$  ( $\gamma_c^- < \gamma < \gamma_c^+$ ), the epidemic is extinct; for  $\gamma > \gamma_c^+$ , the epidemic survives again. A motion-supercritical instance of this situation is given in Table 6 (where  $\mu \sim 3.14$  and  $\beta = 3 > \beta_0$ ).

**Motion-sensitive and Boolean-supercritical example** In this region, for  $\gamma$  equal to 0, there is survival; for small but positive values of  $\gamma$  (more precisely, for  $0 <$

$\gamma$	2.6	2.7	3.3	8.2	8.3	8.6	10	$\infty$
$p_{\text{sim}}$								
$p_{\text{p-b1i}}$	0	$3 \cdot 10^{-4}$		$2 \cdot 10^{-2}$	$2 \cdot 10^{-2}$	$2 \cdot 10^{-2}$	0.045	
$p_{\text{p-b1g1}}$	0	0	$7 \cdot 10^{-5}$	$2 \cdot 10^{-2}$	$2 \cdot 10^{-2}$	$2 \cdot 10^{-2}$	0.045	
$p_{\text{p-m2bi}}$	0	0	0	$4 \cdot 10^{-4}$	$2 \cdot 10^{-3}$	$6 \cdot 10^{-4}$	0.045	

Table 6: Effect of mobility. Below percolation, recovery rate close to  $\mu$ . Fraction of infected nodes ( $p$ ) obtained by simulation, the functional fixed point equation and the polynomial equation. This is for  $\beta = 3$ ,  $a = 1$ ,  $\lambda = 1$  and  $\alpha = 1$ , so that  $\mu \sim 3.14$ . No simulation results are possible for this case. According to p-b1i, the threshold is  $\gamma_c^+ \sim 2.65$ . According to p-b1g1, the threshold is  $\gamma_c^+ \sim 3.12$ . According to p-m2bi, the threshold is  $\gamma_c^+ \sim 8.15$ . So again m2bi is more resistant to the epidemic than m1bi; b1g1 is intermediate.

$\gamma < \gamma_c(\beta)$  with  $\gamma_c(\beta) > 0$ ), there is extinction; from  $\gamma_c$  on, one starts having survival and, above this value, the fraction of infected nodes is strictly increasing in  $\gamma$ . In other words, in this case, *moderate motion stops the survival present in the no-motion case*. One possible explanation is that, in the no-motion Boolean-supercritical case, the persistence of well connected clusters helps maintaining the epidemic and motion dissolves these clusters and makes it more challenging for the epidemic to survive. For high enough values of  $\gamma$ , motion again helps for survival. This situation is illustrated in Figures 4 and 7.

### 5.7.2 Comparison of heuristics

In this subsection, we numerically compare the various heuristics.

The estimates of  $\mu_0$  are 0.263 for b1i, 0.306 for b1g1, and 0.343 for m2bi. Table 7 compares  $\beta_0(\mu)$  for  $\mu > \mu_0$  for the various heuristics. Table 8 compares  $\gamma_c(\mu, \beta)$  for the three heuristics. Table 9 compares  $\gamma_0$  for the three heuristics. Finally, Table 10 compares  $\beta_c$  for the three heuristics.

### 5.7.3 Simulation close to criticality

Simulating the SIS evolution close to criticality is a challenge. By definition, the criticality region is that with a vanishing fraction of infected nodes. By construction the behavior of the epidemic in this region is very sensitive to the size of the torus. Consider parameters such that the infinite system exhibits survival. For all finite size tori with these parameters, the epidemic ends up dying out in finite time, and random fluctuations make this time shorter when decreasing the size of the torus. Since there is no way to simulate arbitrarily large tori, there is hence no direct

$\alpha\mu$	0.5	1	5	10	20
$\beta_{0,\text{sim}}$				> 8.5	
$\beta_{0,\text{p-b1i}}$	0.291	0.796	4.798	9.798	19.798
$\beta_{0,\text{p-b1g1}}$	0.265	0.772	4.777	9.777	19.777
$\beta_{0,\text{p-m2bi}}$	0.157	0.657	4.657	9.657	19.657

Table 7: Threshold  $\beta_0$ . Below  $\beta_0$  there is survival for all motions. Above  $\beta_0$  one needs high enough motion for the epidemic to survive. This is for  $\alpha = 1$ . For this controllability criterion, m2bi is more resistant than b1i and b1g1 is intermediate.

$\beta$	4.75	4.80	4.85	4.90	4.95
$\gamma_{c,\text{sim}}$					
$\gamma_{c,\text{p-b1i}}$	0	3.298	8.824	17.517	42.711
$\gamma_{c,\text{p-b1g1}}$	0	6.265	10.808	19.379	44.557
$\gamma_{c,\text{p-m2bi}}$	5.417	8.042	12.290	20.680	45.720

Table 8: Threshold  $\gamma_c$  for  $\beta > \beta_0$ . Below  $\gamma_c$  there is extinction, above, there is survival. This is for  $\alpha = 1$  and  $\mu = 5$ . Once more, m2bi is more resistant than b1g1 which is more resistant than b1i.

$\alpha\mu$	0.5	1	5	10	20
$\gamma_{0,\text{sim}}$					
$\gamma_{0,\text{p-b1i}}$	0.158	0.450	2.514	5.599	11.309
$\gamma_{0,\text{p-b1g1}}$	0.121	0.370	2.467	4.857	9.818
$\gamma_{0,\text{p-m2bi}}$	0.055	0.232	1.647	3.417	6.955

Table 9: Threshold  $\gamma_0$  when  $\mu > \mu_0$ . Below  $\gamma_0$ ,  $\beta_c = \beta_0$  and survival/extinction is insensitive to  $\gamma$ . This is for  $\alpha = 1$ . We see that m2bi is more sensitive to gamma than b1g1, which is in turn more sensitive than b1i.

way of checking by simulation where the exact value of the critical parameters are located in general.

Here are however two natural ways to assess where the threshold lies, which are both based on the *Mean Time Till Absorption* (MTTA) and which are used to derive the values in the tables of the last sections.

The MTTA is a function of the parameter of interest (say  $\gamma$ ), the torus side, say  $L$ , and the initial condition. To normalize things, we take as initial condition that with all nodes infected. The first method to separate the subcritical and the supercritical regions consists in fixing a large  $L$  and in checking the value of the

$\gamma$	0.2	1	5	10	100	$\infty$
$\beta_{c,\text{sim}}$						
$\beta_{c,\text{p-b1i}}$	4.798	4.798	4.814	4.859	4.976	5
$\beta_{c,\text{p-b1g1}}$	4.932	4.811	4.802	4.854	4.976	5
$\beta_{c,\text{p-m2bi}}$	4.657	4.657	4.740	4.826	4.976	5

Table 10: Threshold  $\beta_c(\gamma)$  slightly above Boolean-percolation ( $\alpha = 1$  and  $\mu = 5$ ). For  $\beta < \beta_c$  there is survival. For  $\beta > \beta_c$ , there is extinction. The function  $\beta_c$  is constant equal to  $\beta_0$  for  $\gamma < \gamma_0$  and increases otherwise. Results are quite close with here b1g1 more resistant than b1i and b1i more resistant than m2bi.

parameter for which there is a clear inflection of the MTTA. The second one leverages the idea that the MTTA should grow slowly with  $L$  in the subcritical case (e.g., logarithmically on a grid) and fast in the supercritical case (e.g. exponentially on a grid). Unfortunately, the exact behavior of the MTTA on a torus is not known, so that this method cannot be used for a proof at this stage.

**Example of estimate of  $\beta_c$**  The setting is that of Table 11. That is  $\mu = 5$  and  $\gamma = 1$ . Note that  $(\mu, \gamma)$  belongs to UMI region and to the Boolean-percolation region.

$\beta$	0	.2	1	2	2.5	2.78	2.86	2.88	2.95
$p_{\text{sim}}$	1	0.92	0.59	0.22	0	0	0	0	0
$p_{\text{p-b1i}}$		0.915	0.598	0.254	0.103	0.028	0.011	0.007	0
$p_{\text{p-b1g1}}$		0.921	0.609	0.264	0.109	0.029	0.011	0.006	0
$p_{\text{p-m2bi}}$	1	0.918	0.605	0.254	0.092	0.006	0	0	0
$p_{\text{p-m}\infty\text{bi}}$		0.92	0.61	0.27	0.12	0.046	0.028	0	0

Table 11: Effect of recovery rate  $\beta$ . Below Boolean-percolation, medium mobility. Fraction of infected nodes ( $p$ ) obtained by simulation, the functional fixed point equation and the polynomial equation. This is for  $\gamma = 1$ ,  $a = 1$ ,  $\lambda = 1$  and  $\alpha = 1$ , so that  $\mu \sim 3.14$ . According to p-b1i,  $\beta_c \sim 2.94$  (2.93 for p-b1g1). According to p-m2bi,  $\beta_c \sim 2.82$ . So, for these values, m2bi is a bit more 'resistant' to the epidemic than b1i. The simulator yields an estimate for this threshold around 2.7 (see Subsection 5.7.3). Note that the three estimates by b1 and m2bi are quite close and consistent with simulation.

Figure 8 illustrates the two methods. Both give a  $\beta_c$  between 2.5 and 2.6. We recall that according to p-b1i,  $\beta_c \sim 2.94$  (2.93 for p-b1g1) and according to

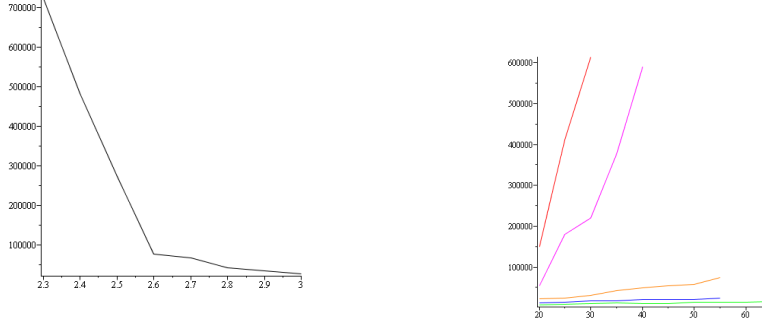


Figure 8: Left: illustration of Method 1 (dependency on the parameter  $\beta$ ); the  $x$  axis features  $\beta$ ; the  $y$  axis features the average of the MTTA over  $L = 20, 25, 30$  and over 20 runs of simulation for each case. Right: illustration of Method 2 (dependency on the torus side  $L$ ): on the  $x$  axis,  $L$ ; on the  $y$  axis, the average of the MTTA; the green curve is for  $\beta = 3$ ; the blue curve is for  $\beta = 2.8$ ; the orange curve is for  $\beta = 2.6$ ; the pink curve is for  $\beta = 2.4$ ; the red curve is for  $\beta = 2.3$ ; All curves are for  $\gamma = 1$ ,  $a = 1$ ,  $\lambda = 1$  and  $\alpha = 1$ , so that  $\mu \sim 3.14$ .

p-m2bi,  $\beta_c \sim 2.82$ .

**Examples of estimate of  $\gamma_c$**  The first example is in the UMS region. The setting is that of Table 8 with  $\alpha = 1$ ,  $\beta = 4.8$  and  $\mu = 5$ . For p-b1i,  $\gamma_c^+ \sim 3.3$  (6.3 for p-b1g1), while for p-m2bi,  $\gamma_c^+ \sim 8.0$ . When using the methodology described above, simulation suggests a value of  $\gamma_c^+$  around 3 (see Figure 9 left). For  $\gamma_c^-$ , the value predicted by p-mb2i is 0.36 and that by p-bli 2.3, while simulation suggests a value around 0.4 (Figure 9 right).

The second example is in the motion-subcritical UMS region. The setting is  $\mu = 1/4$  ( $\lambda = 1/\pi$ ,  $a = 1/2$ ),  $\alpha = 1$ , and  $\beta = 1/5$ . The value of  $\gamma_c^+$  predicted by p-bli is 1.73. That predicted by p-mb2i is 1.84. When using the methodology described above, Method 1 suggests a value of  $\gamma_c^+$  around 2.5 (see Figure 10, left). For  $\gamma_c^-$ , the value predicted by p-mb2i is 0.003 and that by p-bli 0.007. Simulation suggests a value of  $\gamma_c^-$  around 0.1 (see Figure 10, right).

Method 2 is illustrated for  $\gamma_c^-$  and the same case on Fig. 11.

Let us stress once more that none of these methods provides a proof of the  $(\mu, \gamma)$ -phase diagram. Nevertheless, we can deduce from Method 1 (together with confidence intervals) that in the UMS region, the MTTA in a large torus is a decreasing function of  $\gamma$  around  $\gamma_c^-$  and an increasing function of  $\gamma$  around  $\gamma_c^+$ . The



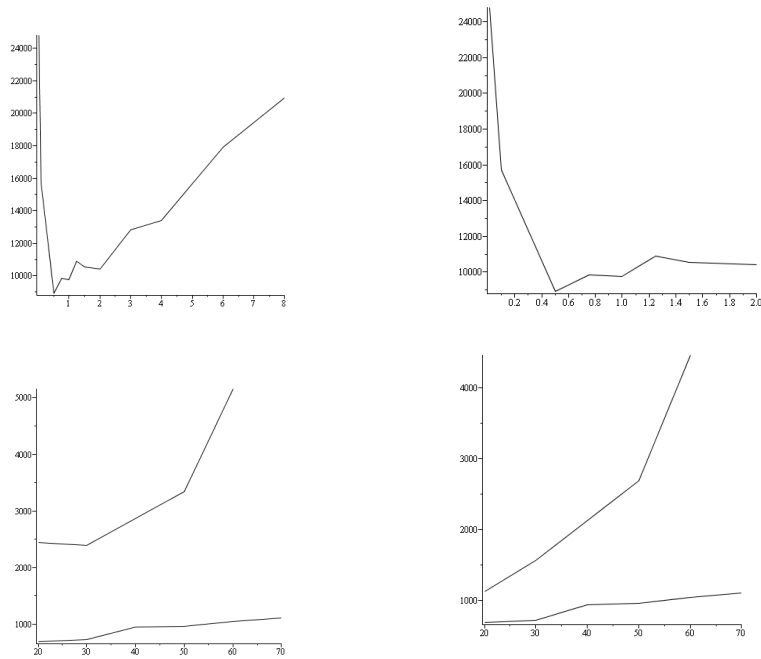


Figure 9: Here,  $\beta = 4.8$ ,  $\alpha = 1$  and  $\mu = 5$ , with  $\lambda = 1$ ,  $a = 1.261$ . Top: Illustration of Method 1 (dependency on the parameter  $\gamma$ ). On the  $x$  axis,  $\gamma$ . On the  $y$  axis, the MTTA averaged out over the cases  $L = 40$  and  $L = 50$ . Left: whole curve. Right: region for the evaluation of  $\gamma_c^-$ . Bottom: Illustration of Method 2: On the  $x$  axis,  $L$ . On the  $y$  axis, the MTTA averaged out over 10 samples. Left: the top curve is for  $\gamma = 0.001$ , the bottom one for  $\gamma = 0.5$ . Right: the top curve is for  $\gamma = 15$ , the bottom one for  $\gamma = 0.5$ .

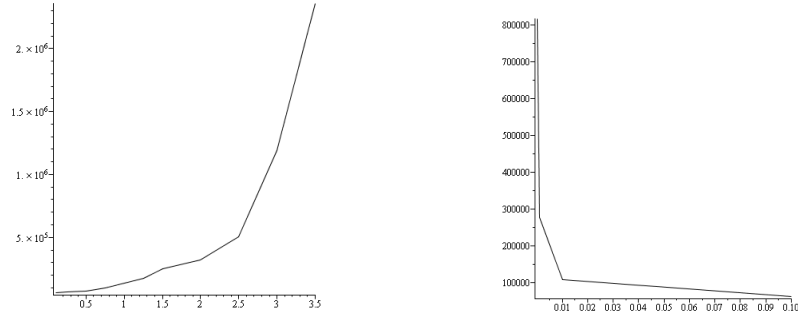


Figure 10: Here,  $\beta = 0.2$ ,  $\alpha = 1$  and  $\mu = 0.25$ , with  $\lambda = 1/\pi$ ,  $a = 1/2$ . Illustration of Method 1 (dependency on the parameter  $\gamma$ ). On the  $x$  axis,  $\gamma$ . On the  $y$  axis, the MTTA averaged out over the cases  $L = 40$  and  $L = 50$ . Left: region for the evaluation of  $\gamma_c^+$ . Right: region for the evaluation of  $\gamma_c^-$ .

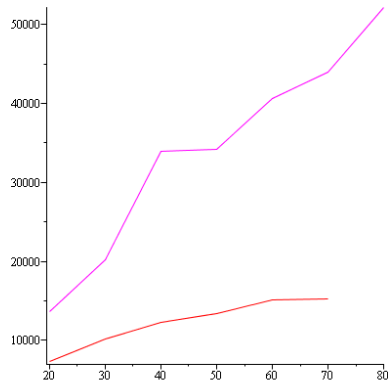


Figure 11: Here,  $\beta = 0.2$ ,  $\alpha = 1$  and  $\mu = 0.25$ , with  $\lambda = 1/\pi$ ,  $a = 1/2$ . Illustration of Method 2 (dependency on the parameter  $\gamma$ ) for  $\gamma_c^-$ . On the  $x$  axis,  $L$ . On the  $y$  axis, the MTTA averaged out over 10 runs. The upper curve is for  $\gamma = 0.001$ ; the lower one is for  $\gamma = 1$ .

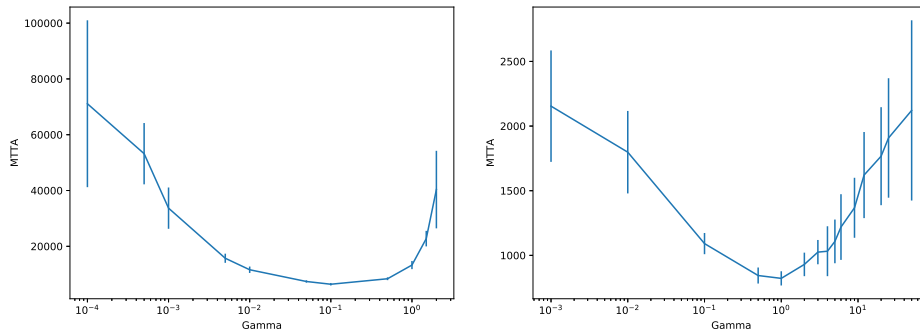


Figure 12: Left: the parameters are those of Figure 9:  $\beta = 4.8$ ,  $\alpha = 1$  and  $\mu = 5$ , with here  $\lambda = 0.8$ ,  $a = 1.41$ . The torus side is  $L = 40$ . Right: the parameters are those of Figure 9:  $\beta = .2$ ,  $\alpha = 1$  and  $\mu = .25$ , with here  $\lambda = 1/\pi$ ,  $a = 1/2$ . The torus side is  $L = 40$ . In both cases, the  $x$ -axis gives the log of  $\gamma$ . The  $y$  axis gives the MTTA with 95% confidence intervals. The MTTA is a unimodal function which decreases around  $\gamma_c^-$  and increases around  $\gamma_c^+$ .

former property in itself is a surprising fact. We illustrate this using 95% confidence intervals in Figure 12.

The physical explanation is that already mentioned: due to the randomness of the configurations, there are clusters with high connectivity; for lower motion rates, these clusters persist for a longer time, which in turn favors the survival of the epidemic.

## 6 No-Motion Case

One option to study the case without motion is to fix  $\gamma$  to 0 in the equations of the last section. This approach suffers of a weakness; it does not allow one to incorporate the fact that the steady state is necessarily the empty measure on the finite components of the Boolean model.

We will hence follow another way below which consists in looking at the epidemic on the infinite cluster of the Boolean model. The reason is that this is a more precise formulation of the problem, given that the underlying graph is not connected and that the epidemic dies out in finite time on any finite connected component.

In this section, the Poisson point process is  $\Xi = \Xi_0$  at all times, with  $\Xi$  of intensity  $\lambda$ . The infinite cluster of the associated Boolean model is denoted by

$\tilde{\Xi}$ . The infected and susceptible sub-point processes of  $\tilde{\Xi}$  are denoted by  $\tilde{\Phi}$  and  $\tilde{\Psi}$ , respectively. That is, the Poisson point process is decomposed into three point processes rather than two: those in finite clusters, say  $\Pi$  (whose state is hence 0 in the stationary regime), those infected and in the infinite cluster,  $\tilde{\Phi}$ , and those susceptible and in the infinite cluster,  $\tilde{\Psi}$ . We have

$$\Xi = \Pi + \tilde{\Xi}, \quad \tilde{\Xi} = \tilde{\Phi} + \tilde{\Psi}.$$

The intensity of  $\Pi$  is  $\lambda(1 - q)$  (the probability for the origin of the Poisson point process to be in a finite cluster under Palm), whereas that of  $\tilde{\Xi}$  is  $\tilde{\lambda} = \lambda q$ . When denoting by  $\tilde{p}$  the steady state fraction of infected nodes in  $\tilde{\Xi}$ , we have that  $\tilde{\Phi}$  and  $\tilde{\Psi}$  have intensities  $\tilde{\lambda}\tilde{p}$  and  $\tilde{\lambda}(1 - \tilde{p})$  respectively.

Let us now give the special forms of the pair correlation functions of these processes. We have

$$1 = (1 - q)^2 \xi_{\Pi, \Pi}(r) + q^2 \xi_{\tilde{\Xi}, \tilde{\Xi}}(r) + 2q(1 - q) \xi_{\Pi, \tilde{\Xi}}(r), \quad \forall r,$$

with also

$$\xi_{\Pi, \tilde{\Xi}}(r) = 0, \quad \text{for } r < a.$$

Hence

$$\begin{aligned} q^2(\tilde{p}^2 \xi_{\tilde{\Phi}, \tilde{\Phi}}(r) + (1 - \tilde{p})^2 \xi_{\tilde{\Psi}, \tilde{\Psi}}(r) + 2\tilde{p}(1 - \tilde{p}) \xi_{\tilde{\Psi}, \tilde{\Phi}}(r)) \\ = q^2 \xi_{\tilde{\Xi}, \tilde{\Xi}}(r) \\ = 1 - (1 - q)^2 \xi_{\Pi, \Pi}(r) \quad \text{for } r < a. \end{aligned}$$

The  $\xi_{\tilde{\Xi}, \tilde{\Xi}}(\cdot)$  function that shows up in the last equation has nothing to do with the SIR dynamics. It only depends on the random graph on which the epidemic develops, namely on the parameters  $\lambda$  and  $f$ . We are only interested in this function above percolation. See Appendix 9.2 for branching type estimates of the parameter  $q$ .

Note that when we are way above the percolation threshold, the infinite cluster is well approximated by the Poisson point process so that taking  $\xi_{\tilde{\Xi}, \tilde{\Xi}}(r) \sim 1$  should be a good approximation.

The main questions of interest on the case where the Boolean model percolates are again the estimation of the critical functions  $\alpha_c$  and  $\beta_c$  and the estimation of the density  $\tilde{p}$  of infected nodes in any stationary regime.

## 6.1 Rate Conservation Principle for Intensities

Consider the case where the Boolean model is supercritical. We can then give another version of Lemma 2 on the infinite cluster  $\tilde{\Xi}$ .

Below we will use the notation  $\tilde{\mu} = \tilde{\lambda}\pi a^2$ . Note the following relations with the earlier notation:

$$\tilde{\lambda} = q\lambda, \quad \tilde{\mu} = q\mu, \quad p = q\tilde{p}. \quad (77)$$

With this notation, we have:

**Lemma 8.** *In the no-motion, Boolean-supercritical case*

$$\tilde{p}\beta = (1 - \tilde{p})\mathbb{E}_{\tilde{\Psi}}^0[I_{\tilde{\Phi}}(0)]. \quad (78)$$

In the no-motion, Boolean-supercritical case, if the  $(\tilde{\Phi}, \tilde{\Psi})$  repulsion property holds (this is not conjectured here), we have

$$\alpha_c \geq \frac{\beta}{\tilde{\mu}}, \quad \beta_c \leq \alpha\tilde{\mu}. \quad (79)$$

If it is not 0, the fraction  $\tilde{p}$  of infected points of  $\tilde{\Xi}$  satisfies the bound

$$0 < \tilde{p} \leq 1 - \frac{\beta}{\alpha\tilde{\mu}}. \quad (80)$$

Note that the  $(\tilde{\Phi}, \tilde{\Psi})$  repulsion property (on the infinite cluster) is not a corollary of that on  $(\Phi, \Psi)$ , namely on the Poisson point process. This second repulsion property possibly only holds in special cases (and is not conjectured). The intuitive reason is that the substrate point process (the infinite cluster) exhibits attraction, which may dominate the repulsion between infected and susceptible. Note that if this cluster repulsion property does not hold, we still have the bounds (10) under the first repulsion conjecture.

Here is the pair-correlation function reformulation of RCP1 on the infinite cluster:

$$\beta = \tilde{\lambda}(1 - \tilde{p})2\pi \int_{\mathbb{R}^+} \xi_{\tilde{\Psi}, \tilde{\Phi}}(r) f(r) r dr. \quad (81)$$

## 6.2 Second Moment RCP

We write the conservation equations for the second order moment measures. The justification is the same as in [2].

$(\tilde{\Phi}, \tilde{\Phi})$  The "mass birth rate" in  $\rho_{\tilde{\Phi}, \tilde{\Phi}}^{(2)}(r)$  is

$$2\rho_{\tilde{\Psi}, \tilde{\Phi}}^{(2)}(r) \left( f(r) + \int_{\mathbb{R}^2} \mu(\tilde{\Phi})_{\tilde{\Psi}, \tilde{\Phi}}^{0,r}(x) f(\|x\|) dx \right),$$

with  $\mu(\tilde{\Phi})_{\tilde{\Psi}, \tilde{\Phi}}^{0,r}(x)$  the conditional density of  $\tilde{\Phi}$  at  $x$  given that  $\tilde{\Psi}$  has a points at  $(0, 0)$  and  $\tilde{\Phi}$  a point at  $(r, 0)$ . The 2 comes from the fact that the infection of the point of  $\tilde{\Psi}$  creates two infected points at a distance  $r$  of each other. The "mass death rate" in  $\rho_{\tilde{\Phi}, \tilde{\Phi}}^{(2)}(r)$  is

$$2\rho_{\tilde{\Phi}, \tilde{\Phi}}^{(2)}(r)\beta.$$

Hence

$$\begin{aligned} & \tilde{\lambda}^2 \tilde{p}^2 \xi_{\tilde{\Phi}, \tilde{\Phi}}(r)\beta \\ &= \tilde{\lambda}^2 \tilde{p}(1 - \tilde{p}) \xi_{\tilde{\Psi}, \tilde{\Phi}}(r) \left( f(r) + \int_{\mathbb{R}^2} \mu(\tilde{\Phi})_{\tilde{\Psi}, \tilde{\Phi}}^{0,r}(x) f(\|x\|) dx \right). \end{aligned} \quad (82)$$

$(\tilde{\Psi}, \tilde{\Psi})$  The "mass birth rate" in  $\rho_{\tilde{\Psi}, \tilde{\Psi}}^{(2)}(r)$  is

$$2\rho_{\tilde{\Psi}, \tilde{\Psi}}^{(2)}(r)\beta.$$

The "mass death rate" in  $\rho_{\tilde{\Psi}, \tilde{\Psi}}^{(2)}(r)$  is

$$2\rho_{\tilde{\Psi}, \tilde{\Psi}}^{(2)}(r) \int_{\mathbb{R}^2} \mu(\tilde{\Phi})_{\tilde{\Psi}, \tilde{\Psi}}^{0,r}(x) f(\|x\|) dx,$$

with a similar notation. Hence

$$\begin{aligned} & \tilde{\lambda}^2 \tilde{p}(1 - \tilde{p}) \xi_{\tilde{\Psi}, \tilde{\Phi}}(r)\beta \\ &= \tilde{\lambda}^2 (1 - \tilde{p})^2 \xi_{\tilde{\Psi}, \tilde{\Psi}}(r) \int_{\mathbb{R}^2} \mu(\tilde{\Phi})_{\tilde{\Psi}, \tilde{\Psi}}^{0,r}(x) f(\|x\|) dx. \end{aligned} \quad (83)$$

$(\tilde{\Psi}, \tilde{\Phi})$  The "mass birth rate" in  $\rho_{\tilde{\Psi}, \tilde{\Phi}}^{(2)}(r)$  is

$$2\rho_{\tilde{\Phi}, \tilde{\Phi}}^{(2)}(r)\beta + 2\rho_{\tilde{\Psi}, \tilde{\Psi}}^{(2)}(r) \int_{\mathbb{R}^2} \mu(\tilde{\Phi})_{\tilde{\Psi}, \tilde{\Psi}}^{0,r}(x) f(\|x\|) dx.$$

The "mass death rate" in  $\rho_{\tilde{\Psi}, \tilde{\Phi}}^{(2)}(r)$  is

$$2\rho_{\tilde{\Psi}, \tilde{\Phi}}^{(2)}(r)\beta + 2\rho_{\tilde{\Psi}, \tilde{\Phi}}^{(2)}(r) \left( f(r) + \int_{\mathbb{R}^2} \mu(\tilde{\Phi})_{\tilde{\Psi}, \tilde{\Phi}}^{0,r}(x) f(\|x\|) dx \right),$$

with the same type of notation. So

$$\begin{aligned} \tilde{\lambda}^2 \tilde{p}^2 \xi_{\tilde{\Phi}, \tilde{\Phi}}(r) \beta + \tilde{\lambda}^2 (1 - \tilde{p})^2 \xi_{\tilde{\Psi}, \tilde{\Psi}}(r) \int_{\mathbb{R}^2} \mu(\tilde{\Phi})_{\tilde{\Psi}, \tilde{\Psi}}^{0,r}(x) f(\|x\|) dx = & \quad (84) \\ \tilde{\lambda}^2 \tilde{p} (1 - \tilde{p}) \xi_{\tilde{\Psi}, \tilde{\Phi}}(r) \beta + \tilde{\lambda}^2 \tilde{p} (1 - \tilde{p}) \xi_{\tilde{\Psi}, \tilde{\Phi}}(r) \left( f(r) + \int_{\mathbb{R}^2} \mu(\tilde{\Phi})_{\tilde{\Psi}, \tilde{\Phi}}^{0,r}(x) f(\|x\|) dx \right). & \end{aligned}$$

We see that (84) is obtained by linear combination of (82) and (83).

**Theorem 9.** *If there exists a stationary regime, then the stationary pair correlation functions satisfy the following system of integral equations:*

$$\begin{aligned} \tilde{p} \beta \xi_{\tilde{\Phi}, \tilde{\Phi}}(r) &= (1 - \tilde{p}) \xi_{\tilde{\Psi}, \tilde{\Phi}}(r) \left( f(r) + \int_{\mathbb{R}^2} \mu(\tilde{\Phi})_{\tilde{\Psi}, \tilde{\Phi}}^{0,r}(x) f(\|x\|) dx \right) \\ \tilde{p} \beta \xi_{\tilde{\Psi}, \tilde{\Phi}}(r) &= (1 - \tilde{p}) \xi_{\tilde{\Psi}, \tilde{\Psi}}(r) \int_{\mathbb{R}^2} \mu(\tilde{\Phi})_{\tilde{\Psi}, \tilde{\Psi}}^{0,r}(x) f(\|x\|) dx, \end{aligned} \quad (85)$$

with  $\mu(\tilde{\Phi})_{\tilde{\Psi}, \tilde{\Psi}}^{0,r}(x)$  and  $\mu(\tilde{\Phi})_{\tilde{\Psi}, \tilde{\Phi}}^{0,r}(x)$  the conditional densities defined above.

The last system can be complemented by the following relations, which were established above:

$$\beta = (1 - \tilde{p}) \tilde{\lambda} \int_{\mathbb{R}^2} \xi_{\tilde{\Psi}, \tilde{\Phi}}(x) f(\|x\|) dx \quad (86)$$

and

$$\tilde{p}^2 \xi_{\tilde{\Phi}, \tilde{\Phi}}(r) + (1 - \tilde{p})^2 \xi_{\tilde{\Psi}, \tilde{\Psi}}(r) + 2\tilde{p}(1 - \tilde{p}) \xi_{\tilde{\Psi}, \tilde{\Phi}}(r) = c(r), \quad (87)$$

where  $c(\cdot)$  denotes the pair correlation function of the infinite component of the Boolean cluster:

$$c(r) := \xi_{\tilde{\Xi}, \tilde{\Xi}}(r), \quad (88)$$

under the assumption of Boolean-percolation.

Note that once the pair correlation functions solution of this system are determined, we get the fraction of infected nodes  $p$  in the Poisson point process of intensity  $\lambda$  from (77) and (86) through the relation

$$p = q\tilde{p} = q - \frac{\beta}{\lambda \int_{\mathbb{R}^2} \xi_{\tilde{\Psi}, \tilde{\Phi}}(x) f(\|x\|) dx}. \quad (89)$$

### 6.3 Heuristics

Below, we use the methodology and classification of Sections 5.2 and 5.3.

### 6.3.1 Heuristic B1I

**Functional equation f-b1i** The functional equation reads

$$\begin{aligned}
\tilde{p}\xi_{\tilde{\Phi},\tilde{\Phi}}(r)\beta &= (1 - \tilde{p})\xi_{\tilde{\Psi},\tilde{\Phi}}(r)f(r) \\
&\quad + \tilde{\lambda}(1 - \tilde{p})\tilde{p}\xi_{\tilde{\Psi},\tilde{\Phi}}(r)^{\frac{2}{3}} \int_{\mathbb{R}^2} \xi_{\tilde{\Psi},\tilde{\Phi}}(\|\mathbf{x}\|)^{\frac{2}{3}} \xi_{\tilde{\Phi},\tilde{\Phi}}(\|\mathbf{x} - (\mathbf{r}, \mathbf{0})\|)^{\frac{2}{3}} f(\|\mathbf{x}\|) d\mathbf{x} \\
\xi_{\tilde{\Psi},\tilde{\Phi}}(r)\beta &= \tilde{\lambda}(1 - \tilde{p})\xi_{\tilde{\Psi},\tilde{\Psi}}(r)^{\frac{2}{3}} \int_{\mathbb{R}^2} \xi_{\tilde{\Psi},\tilde{\Phi}}(\|\mathbf{x}\|)^{\frac{2}{3}} \xi_{\tilde{\Psi},\tilde{\Phi}}(\|\mathbf{x} - (\mathbf{r}, \mathbf{0})\|)^{\frac{2}{3}} f(\|\mathbf{x}\|) d\mathbf{x}.
\end{aligned} \tag{90}$$

### Iterative Scheme s-b1i

**Polynomial equation p-b1i** Under the conditions for the polynomial setting, we get the p-b1 polynomial system

$$\begin{aligned}
\beta\tilde{p}v &= \alpha(1 - \tilde{p})w + \beta\tilde{p}v^{\frac{2}{3}}w^{\frac{1}{3}} \\
w^{\frac{2}{3}} &= z^{\frac{2}{3}}.
\end{aligned}$$

Since  $w$  and  $z$  are positive, we get  $z = w$ . Hence,

$$\begin{aligned}
\beta\tilde{p}v &= \alpha(1 - \tilde{p})w + \beta\tilde{p}v^{\frac{2}{3}}w^{\frac{1}{3}} \\
w(1 - \tilde{p})^2 &= c - \tilde{p}^2v - 2\tilde{p}(1 - \tilde{p})w
\end{aligned} \tag{91}$$

and we get the following polynomial system (at the cost of introducing spurious solutions)

$$\begin{aligned}
v^2w(\alpha\tilde{\mu}w - \beta)^3 &= (v(\alpha\tilde{\mu}w - \beta) - w)^3 \\
v(\alpha\tilde{\mu}w - \beta)^2 &= w(\alpha\tilde{\mu}w(c\alpha\tilde{\mu} - 2\beta) + \beta^2).
\end{aligned} \tag{92}$$

**Critical values** Let us look at what happens when  $\tilde{p}$  tends to 0. It follows from the first moment equation that  $w$  tends to  $\frac{\beta}{\alpha\tilde{\mu}}$ , and from the second equation in (91) that the associated critical value of  $\beta$  is  $\beta_c = c\alpha\tilde{\mu} = \alpha c q \mu$ .

We conclude that according to p-b1i, in the no-motion case, for all fixed  $\beta$ ,  $\lambda$  and  $a$  such that the Boolean model with parameters  $(\lambda, a)$  is supercritical,  $\beta_c = \alpha c q \mu$ .



### 6.3.2 Heuristic G1

#### Functional equation f-g1

$$\begin{aligned}
\tilde{p}\xi_{\tilde{\Phi},\tilde{\Phi}}(r)\beta &= (1 - \tilde{p})\xi_{\tilde{\Psi},\tilde{\Phi}}(r)f(r) \\
&\quad + \tilde{\lambda}(1 - \tilde{p})\tilde{p}\xi_{\tilde{\Psi},\tilde{\Phi}}(r) \int_{\mathbb{R}^2} \xi_{\tilde{\Psi},\tilde{\Phi}}(\|\mathbf{x}\|)^{\frac{1}{2}} \xi_{\tilde{\Phi},\tilde{\Phi}}(\|\mathbf{x} - (\mathbf{r}, \mathbf{0})\|)^{\frac{1}{2}} f(\|\mathbf{x}\|) d\mathbf{x} \\
\xi_{\tilde{\Psi},\tilde{\Phi}}(r)\beta &= \tilde{\lambda}(1 - \tilde{p})\xi_{\tilde{\Psi},\tilde{\Psi}}(r) \int_{\mathbb{R}^2} \xi_{\tilde{\Psi},\tilde{\Phi}}(\|\mathbf{x}\|)^{\frac{1}{2}} \xi_{\tilde{\Phi},\tilde{\Phi}}(\|\mathbf{x} - (\mathbf{r}, \mathbf{0})\|)^{\frac{1}{2}} f(\|\mathbf{x}\|) d\mathbf{x}.
\end{aligned} \tag{93}$$

**Polynomial equation p-g1** Under the conditions for the polynomial setting, we get the p-g1 polynomial system

$$\begin{aligned}
\beta\tilde{p}v &= \alpha(1 - \tilde{p})w + \beta\tilde{p}v^{\frac{1}{2}}w^{\frac{1}{2}} \\
\beta w &= \beta z.
\end{aligned}$$

This equation coincides with that of p-mb $\infty$ g1 and p-b1g1 and will be studied below (see Equation 108).

### 6.3.3 Heuristic B1G1

**Functional equation f-b1g1** The functional equation reads

$$\begin{aligned}
\tilde{p}\xi_{\tilde{\Phi},\tilde{\Phi}}(r)\beta &= (1 - \tilde{p})\xi_{\tilde{\Psi},\tilde{\Phi}}(r)f(r) \\
&\quad + \lambda(1 - \tilde{p})\tilde{p}\xi_{\tilde{\Psi},\tilde{\Phi}}(r)^{\frac{5}{6}} \int_{\mathbb{R}^2} \xi_{\tilde{\Psi},\tilde{\Phi}}(\|\mathbf{x}\|)^{\frac{2}{3}} \xi_{\tilde{\Phi},\tilde{\Phi}}(\|\mathbf{x} - (\mathbf{r}, \mathbf{0})\|)^{\frac{1}{2}} f(\|\mathbf{x}\|) d\mathbf{x} \\
\xi_{\tilde{\Psi},\tilde{\Phi}}(r)\beta &= \tilde{\lambda}(1 - \tilde{p})\xi_{\tilde{\Psi},\tilde{\Psi}}(r)^{\frac{1}{2}} \int_{\mathbb{R}^2} \xi_{\tilde{\Psi},\tilde{\Phi}}(\|\mathbf{x}\|)^{\frac{5}{6}} \xi_{\tilde{\Phi},\tilde{\Phi}}(\|\mathbf{x} - (\mathbf{r}, \mathbf{0})\|)^{\frac{2}{3}} f(\|\mathbf{x}\|) d\mathbf{x}.
\end{aligned} \tag{94}$$

**Polynomial equation p-b1g1** Under the conditions for the polynomial setting, we get the p-b1g1 polynomial system

$$\begin{aligned}
\beta\tilde{p}v &= \alpha(1 - \tilde{p})w + \beta\tilde{p}v^{\frac{1}{2}}w^{\frac{1}{2}} \\
\beta w &= \beta z^{\frac{1}{2}}w^{\frac{1}{2}}.
\end{aligned}$$

This polynomial equation coincides with that of p-g1 above and that of p-mb $\infty$ g1 below. It will be studied in Equation 108) in the p-mb $\infty$ g1 paragraph.

### 6.3.4 Heuristic M2BI

**Functional equation f-m2bi** Equations (82) and (83) lead to the following system of integral equations (f-m2bi):

$$\begin{aligned}
\tilde{p}\xi_{\tilde{\Phi},\tilde{\Phi}}(r)\beta &= (1 - \tilde{p})\xi_{\tilde{\Psi},\tilde{\Phi}}(r)f(r) \\
&+ \frac{1}{2}\lambda(1 - \tilde{p})\tilde{p}\xi_{\tilde{\Psi},\tilde{\Phi}}(r) \int_{\mathbb{R}^2} \xi_{\tilde{\Psi},\tilde{\Phi}}(\|\mathbf{x}\|)f(\|\mathbf{x}\|)d\mathbf{x} \\
&+ \frac{1}{2}\lambda(1 - \tilde{p})\tilde{p}\xi_{\tilde{\Psi},\tilde{\Phi}}(r)^{\frac{1}{2}} \int_{\mathbb{R}^2} \xi_{\tilde{\Psi},\tilde{\Phi}}(\|\mathbf{x}\|^{\frac{1}{2}}\xi_{\tilde{\Phi},\tilde{\Phi}}(\|\mathbf{x} - \mathbf{r}\|)f(\|\mathbf{x}\|)d\mathbf{x} \\
\xi_{\tilde{\Psi},\tilde{\Phi}}(r)\beta &= \frac{1}{2}\lambda(1 - \tilde{p}) \int_{\mathbb{R}^2} \xi_{\tilde{\Psi},\tilde{\Phi}}(\|\mathbf{x}\|)\xi_{\tilde{\Psi},\tilde{\Phi}}(\|\mathbf{x} - \mathbf{r}\|)f(\|\mathbf{x}\|)d\mathbf{x} \\
&+ \frac{1}{2}\lambda(1 - \tilde{p})\xi_{\tilde{\Psi},\tilde{\Psi}}(r) \int_{\mathbb{R}^2} \xi_{\tilde{\Psi},\tilde{\Phi}}(\|\mathbf{x}\|^{\frac{1}{2}}\xi_{\tilde{\Psi},\tilde{\Phi}}(\|\mathbf{x} - \mathbf{r}\|^{\frac{1}{2}}f(\|\mathbf{x}\|)d\mathbf{x}.
\end{aligned} \tag{95}$$

**Iterative scheme s-m2bi** The system (95) in turn leads to the following iterative integral equation scheme with again the two "state" functions  $\xi_{\tilde{\Phi},\tilde{\Phi}}^{(n)}(\cdot)$  and  $\xi_{\tilde{\Psi},\tilde{\Phi}}^{(n)}(\cdot)$ :

$$\begin{aligned}
\xi_{\tilde{\Phi},\tilde{\Phi}}^{(n+1)}(r) &= \frac{1}{\beta} \frac{1 - \tilde{p}^{(n)}}{\tilde{p}^{(n)}} \xi_{\tilde{\Psi},\tilde{\Phi}}^{(n)}(r)f(r) \\
&+ \frac{1}{2} \frac{\tilde{\lambda}}{\beta} (1 - \tilde{p}^{(n)}) \int_{\mathbb{R}^2} \xi_{\tilde{\Psi},\tilde{\Phi}}^{(n)}(\|\mathbf{x}\|)\xi_{\tilde{\Phi},\tilde{\Phi}}^{(n)}(\|\mathbf{x} - \mathbf{r}\|)f(\|\mathbf{x}\|)d\mathbf{x} \\
&+ \frac{1}{2} \lambda (1 - \tilde{p}^{(n)}) \tilde{p}^{(n)} \xi_{\tilde{\Psi},\tilde{\Phi}}^{(n)}(r) \int_{\mathbb{R}^2} \xi_{\tilde{\Psi},\tilde{\Phi}}^{(n)}(\|\mathbf{x}\|)\xi_{\tilde{\Phi},\tilde{\Phi}}^{(n)}(\|\mathbf{x} - \mathbf{r}\|)f(\|\mathbf{x}\|)d\mathbf{x} \\
\xi_{\tilde{\Psi},\tilde{\Phi}}^{(n+1)}(r) &= \frac{1}{2} \frac{\tilde{\lambda}}{\beta} (1 - \tilde{p}^{(n)}) \int_{\mathbb{R}^2} \xi_{\tilde{\Psi},\tilde{\Phi}}^{(n)}(\|\mathbf{x}\|)\xi_{\tilde{\Psi},\tilde{\Phi}}^{(n)}(\|\mathbf{x} - \mathbf{r}\|)f(\|\mathbf{x}\|)d\mathbf{x} \\
&+ \frac{1}{2} \lambda (1 - \tilde{p}^{(n)}) \xi_{\tilde{\Psi},\tilde{\Psi}}^{(n)}(r) \int_{\mathbb{R}^2} \xi_{\tilde{\Psi},\tilde{\Phi}}^{(n)}(\|\mathbf{x}\|^{\frac{1}{2}}\xi_{\tilde{\Psi},\tilde{\Phi}}^{(n)}(\|\mathbf{x} - \mathbf{r}\|^{\frac{1}{2}}f(\|\mathbf{x}\|)d\mathbf{x}.
\end{aligned} \tag{96}$$

In these equations, we have

$$\tilde{p}^{(n)} = 1 - \frac{\beta}{\tilde{\lambda}2\pi \int_{\mathbb{R}^+} \xi_{\tilde{\Psi},\tilde{\Phi}}^{(n)}(r)f(r)rdr}, \tag{97}$$

and

$$\xi_{\tilde{\Psi},\tilde{\Psi}}^{(n)}(r) = \frac{1}{(1 - \tilde{p}^{(n)})^2} \left( c(r) - (\tilde{p}^{(n)})^2 \xi_{\tilde{\Phi},\tilde{\Phi}}^{(n)}(r) - 2\tilde{p}^{(n)} (1 - \tilde{p}^{(n)}) \xi_{\tilde{\Psi},\tilde{\Phi}}^{(n)}(r) \right) \tag{98}$$

with  $c(r)$  defined in (88).

**Polynomial equation p-m2bi** Under the conditions for the polynomial setting, we get

$$\begin{aligned}\beta\tilde{p}v &= 2\alpha(1-\tilde{p})w + \beta\tilde{p}w \\ \beta w &= \frac{1}{2}\beta w + \frac{1}{2}\beta z.\end{aligned}\quad (99)$$

Since  $w = z$ , (87) reads

$$c = w(1-\tilde{p})^2 + \tilde{p}^2v + 2\tilde{p}(1-\tilde{p})w. \quad (100)$$

The above system can be rewritten as

$$\begin{aligned}(\alpha\tilde{\mu}w - \beta)v &= 2\alpha w + (\alpha\tilde{\mu}w - \beta)w \\ c(\alpha\tilde{\mu}w)^2 &= w\beta^2 + (\alpha\tilde{\mu}w - \beta)^2v + 2(\alpha\tilde{\mu}w - \beta)\beta w.\end{aligned}\quad (101)$$

By eliminating  $v$ , we get

$$(\alpha\tilde{\mu}w - \beta)(\alpha\tilde{\mu}w - \beta + 2\alpha) = c(\alpha\tilde{\mu})^2w - 2(\alpha\tilde{\mu}w - \beta)\beta - \beta^2. \quad (102)$$

**Critical values** When  $p$  tends to 0,  $w$  tends to  $\frac{\beta}{\alpha\tilde{\mu}}$  and it follows from (100) that the associated value of  $\beta$  is  $\beta_c = c\alpha\tilde{\mu}$ . The conclusions are then the same as above.

### 6.3.5 Heuristic $M_{\infty}BI$

**Functional equation f-m $\infty$ bi** The associated functional equation reads

$$\begin{aligned}\tilde{p}\xi_{\tilde{\Phi},\tilde{\Phi}}(r)\beta &= (1-\tilde{p})\xi_{\tilde{\Psi},\tilde{\Phi}}(r)f(r) + \lambda(1-\tilde{p})\tilde{p}\xi_{\tilde{\Psi},\tilde{\Phi}}(r) \\ \int_{\mathbb{R}^2} \int_0^1 \xi_{\tilde{\Psi},\tilde{\Phi}}(\|\mathbf{x}\|)^\eta \xi_{\tilde{\Phi},\tilde{\Phi}}(\|\mathbf{x}-\mathbf{r}\|)^{2(1-\eta)} \xi_{\tilde{\Psi},\tilde{\Phi}}(r)^{\eta-1} f(\|\mathbf{x}\|) d\eta d\mathbf{x} \\ \xi_{\tilde{\Psi},\tilde{\Phi}}(r)\beta &= \tilde{\lambda}(1-\tilde{p})\xi_{\tilde{\Psi},\tilde{\Psi}}(r) \\ \int_{\mathbb{R}^2} \int_0^1 \xi_{\tilde{\Psi},\tilde{\Phi}}(\|\mathbf{x}\|)^\eta \xi_{\tilde{\Phi},\tilde{\Phi}}(\|\mathbf{x}-\mathbf{r}\|)^\eta f(\|\mathbf{x}\|) \xi_{\tilde{\Psi},\tilde{\Psi}}(r)^{1-2\eta} d\eta d\mathbf{x}.\end{aligned}\quad (103)$$

**Polynomial equation p-m $\infty$ bi** The polynomial<sup>4</sup> equation reads

$$\begin{aligned}
\beta\tilde{p}v &= \alpha(1 - \tilde{p})w + \beta\tilde{p}\frac{v^2}{w} \int_0^1 w^{2\eta}v^{-2\eta}d\eta \\
&= \alpha(1 - \tilde{p})w + \beta\tilde{p}\frac{1}{w} \frac{w^2 - v^2}{\log(w^2) - \log(v^2)} \\
\beta\tilde{p}w &= \tilde{p}\beta\frac{z^2}{w} \int_0^1 w^{2\eta}z^{-2\eta}d\eta = \beta\tilde{p}\frac{1}{w} \frac{w^2 - z^2}{\log(w^2) - \log(z^2)} \\
1 - \tilde{p} &= \frac{\beta}{\alpha\tilde{\mu}w} \\
z(1 - \tilde{p})^2 &= c - \tilde{p}^2v - 2\tilde{p}(1 - \tilde{p})w. \tag{104}
\end{aligned}$$

We hence get the system

$$\begin{aligned}
v(\alpha\tilde{\mu}w - \beta) &= \alpha w + (\alpha\tilde{\mu}w - \beta)\frac{1}{w} \frac{w^2 - v^2}{\log(w^2) - \log(v^2)} \\
w^2 &= \frac{w^2 - z^2}{\log(w^2) - \log(z^2)} \\
z &= \frac{1}{\beta^2} (w^2(c\alpha^2\tilde{\mu}^2 - 2\alpha\beta\tilde{\mu}) - (\alpha\tilde{\mu}w - \beta)^2v + 2\beta^2w) \tag{105}
\end{aligned}$$

It is easy to show that the second equation in (105) implies that  $z = w$  as in the earlier cases. So the system p-mb $\infty$  actually reads

$$\begin{aligned}
vw(\alpha\tilde{\mu}w - \beta) &= \alpha w^2 + (\alpha\tilde{\mu}w - \beta)\frac{w^2 - v^2}{\log(w^2) - \log(v^2)} \\
0 &= w^2(c\alpha^2\tilde{\mu}^2 - 2\alpha\beta\tilde{\mu}) - (\alpha\tilde{\mu}w - \beta)^2v + \beta^2w. \tag{106}
\end{aligned}$$

**Critical values** Let us look at what happens when  $p$  tends to 0 in (104). It follows from the third equation that  $w$  tends to  $\frac{\beta}{\alpha\tilde{\mu}}$ , from the last one that  $z$  tends to  $c$ , and from the first one that  $\tilde{p}^2v(\tilde{p})$  tends to  $c - \frac{\beta}{\alpha\tilde{\mu}}$ . Multiplying the first equation by  $p$  and letting  $p$  to 0, we get that necessarily  $c = \frac{\beta}{\alpha\tilde{\mu}}$ . So we have again  $\beta_c = \alpha\tilde{\mu}$ .

---

<sup>4</sup>Polynomial is an abuse of terminology here

### 6.3.6 Heuristic $M_\infty BG1$

**Functional equation f- $m_\infty g1$**  The associated functional equation reads

$$\begin{aligned}
\tilde{p}\xi_{\tilde{\Phi},\tilde{\Phi}}(r)\beta &= (1-\tilde{p})\xi_{\tilde{\Psi},\tilde{\Phi}}(r)f(r) + \lambda(1-\tilde{p})\tilde{p}\xi_{\tilde{\Psi},\tilde{\Phi}}(r) \\
\int_{\mathbb{R}^2} \int_0^1 \xi_{\tilde{\Psi},\tilde{\Phi}}(\|\mathbf{x}\|)^{1-\frac{\eta}{2}} \xi_{\tilde{\Phi},\tilde{\Phi}}(\|\mathbf{x}-\mathbf{r}\|)^{\frac{1}{2}} \xi_{\tilde{\Psi},\tilde{\Phi}}(r)^{\frac{\eta}{2}-\frac{1}{2}} f(\|\mathbf{x}\|) d\eta d\mathbf{x} \\
\xi_{\tilde{\Psi},\tilde{\Phi}}(r)\beta &= \tilde{\lambda}(1-\tilde{p})\xi_{\tilde{\Psi},\tilde{\Psi}}(r) \\
\int_{\mathbb{R}^2} \int_0^1 \xi_{\tilde{\Psi},\tilde{\Phi}}(\|\mathbf{x}\|)^{\frac{1}{2}+\frac{\eta}{2}} \xi_{\tilde{\Phi},\tilde{\Phi}}(\|\mathbf{x}-\mathbf{r}\|)^{1-\frac{\eta}{2}} f(\|\mathbf{x}\|) \xi_{\tilde{\Psi},\tilde{\Psi}}(r)^{-\frac{1}{2}} d\eta d\mathbf{x}.
\end{aligned} \tag{107}$$

**Polynomial equation p- $m_\infty bg1$**  The polynomial<sup>5</sup> equation reads

$$\begin{aligned}
\beta\tilde{p}v &= \alpha(1-\tilde{p})w + \beta\tilde{p}v^{\frac{1}{2}}w^{\frac{1}{2}} \\
\beta\tilde{p}w &= \beta\tilde{p}z^{\frac{1}{2}}w^{\frac{1}{2}} \\
1-\tilde{p} &= \frac{\beta}{\alpha\tilde{\mu}w} \\
z(1-\tilde{p})^2 &= c - \tilde{p}^2v - 2\tilde{p}(1-\tilde{p})w.
\end{aligned} \tag{108}$$

We hence get that  $z = w$ . So

$$\begin{aligned}
\beta\tilde{p}v &= \alpha(1-\tilde{p})w + \beta\tilde{p}v^{\frac{1}{2}}w^{\frac{1}{2}} \\
w(1-\tilde{p})^2 &= c - \tilde{p}^2v - 2\tilde{p}(1-\tilde{p})w.
\end{aligned} \tag{109}$$

**Critical values** Let us look at what happens when  $p$  tends to 0 in (108). It follows from the third equation that  $w$  tends to  $\frac{\beta}{\alpha\tilde{\mu}}$ , from the last one that  $z$  tends to  $c$ . So  $c = \frac{\beta}{\alpha\tilde{\mu}}$ . So we have again  $\beta_c = \alpha\tilde{\mu}$ .

## 6.4 Numerical Results

### 6.4.1 Densities

Table 12 studies a case where the Boolean model is way above percolation (we have  $\tilde{\mu} \sim 12.56 > \tilde{\mu}_c \sim 4.5$ ). Table 13 studies situations where  $\tilde{\mu}$  is close to (but above) the percolation threshold  $\mu_c \sim 4.5$ .

<sup>5</sup>Polynomial is an abuse of terminology here

$\beta$	2	4	8	12
$p_{\text{sim}}$	0.82	0.64	0.26	0
$p_{\text{f-b1i}}$	0.82	0.64	0.33	
$p_{\text{p-b1i}}$	0.80	0.62	0.30	0.020
$p_{\text{p-b1g1}}$	0.81	0.63	0.30	0.022
$p_{\text{p-m2bi}}$	0.81	0.63	0.31	0.020
$p_{\text{p-m}\infty\text{bi}}$	0.82	0.64	0.32	0.032
$p_{\text{hs}}$	0.84	0.67	0.35	0.045

Table 12: No-mobility case. Way above percolation. Fraction of infected nodes ( $\tilde{p}$ ) obtained by simulation, solution of the integral equation, the solution of the polynomial equation, and the high speed (hs) formula (14) Various heuristics are considered. This is for  $a = 2$ ,  $\lambda = 1$  and  $\alpha = 1$ . Prediction is good. It is better when  $p$  is not too close to 0. Note that b1 and m2bi provide similar results.

$\tilde{\mu}$	4.54	4.80	5.31	6.28
$p_{\text{sim}}$	0.07		0.23	0.39
$p_{\text{p-b1i}}$	0.02		0.26	0.41
$p_{\text{p-b1g1}}$	0.03		0.28	0.43
$p_{\text{p-m2bi}}$	0.02		0.27	0.43
$q_{\text{sim}}$	0.86		0.95	0.99

Table 13: No-mobility case. Above and close to the percolation threshold. Fraction of infected nodes ( $\tilde{p}$ ) obtained by simulation, the functional equation and the polynomial equation. This is for  $\alpha = 1$  and  $\beta = 3$ . Prediction is good again, except for very small values of  $p$ , with b1i and m2bi providing quite similar results, which slightly overestimate  $p$ .

#### 6.4.2 Pair correlation functions

The pair correlation functions of Heuristic B1 are depicted in Figure 13.

## 7 Variants

### 7.1 Epidemic Model Variants

In relation with certain epidemics, the basic model described above is unsatisfactory in several ways.

First the SIS dynamics is not sufficient. SIR (or further variants like SEIR) would be more satisfactory.

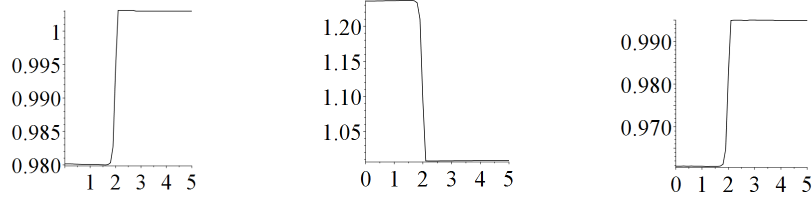


Figure 13: Left: the  $\xi_{\tilde{\Psi}, \tilde{\Phi}}(r)$  function; Center: the  $\xi_{\tilde{\Phi}, \tilde{\Phi}}(r)$  function; Right: the  $\xi_{\tilde{\Psi}, \tilde{\Psi}}(r)$  function. This is Heuristic f-b1.

In addition, individuals should be compartmented in at least two classes, say at risk  $A$  and not at risk  $N$ . Individuals not at risk would go along the SIS cycle (or their variants). In a first model, individuals at risk die when exposed to a high viral charge. For modelling this in the Markov SIS framework, an individual  $X$  of type  $A$  in state  $S$  has a death rate equal to

$$\mathcal{D}(X, \tilde{\Phi}_t) = \sum_{Y \in \tilde{\Phi}_t} g(\|X - Y\|).$$

Here, we could take  $g = f$  or  $g = \delta f$ , with  $\delta$  a positive constant. Another (and more favorable) variant is that where individuals at risk become sick at rate

$$\mathcal{D}(X, \tilde{\Phi}_t) = \sum_{Y \in \Phi_t} g(\|X - Y\|)$$

and where the result of sickness is death with probability  $\nu$  and recovery with probability  $1 - \nu$ . This compartmenting can be combined with SIR or extensions.

Since we will analyze stationary regimes, the compartmental model is more interesting when there is a birth rate of individuals, with births representing either births in the biological sense or arrivals from far away. In the absence of births, all individuals at risk eventually die and the steady state boils down to that of the SIS model for individuals of type  $N$ , namely the basic model. A natural model for births is that of a Poisson rain with intensity  $\lambda$ . Newborns have a given probability to be in any state of  $\{N, A\} \times \{I, S\}$ .

Some of these variants will be discussed in the note. However the basic model will be the basic one.

## 7.2 Far Random Waypoint and Death

One can combine the setting of Section 5 with that of deaths as described in the last subsection. The model features external births with a rate  $\eta$ , with say only

susceptible individuals, migration with a rate  $\gamma$ , and death with probability  $\nu$  upon infection. If  $\nu = \eta = 0$ , we obtain the last model. In this new case, the point process  $\Xi$  (we should say  $\tilde{\Xi}$  but decided to drop the tilde) is not Poisson any longer and both its intensity  $\lambda$  and its pair correlation functions are unknown. The equations are

$$\begin{aligned}
p\xi_{\Phi,\Phi}(r)(\beta + \gamma) &= p\gamma \\
&+ (1-p)(1-\nu)\xi_{\Psi,\Phi}(r) \left( f(r) + \int_{\mathbb{R}^2} \mu(\Phi)_{\Psi,\Phi}^{0,r}(x) f(\|x\|) dx \right) \\
\lambda p\xi_{\Psi,\Phi}(r)\beta + \lambda(1-p)\gamma + \eta &= \\
\lambda(1-p)\xi_{\Psi,\Psi}(r) \left( \gamma + \int_{\mathbb{R}^2} \mu(\Phi)_{\Psi,\Psi}^{0,r}(x) f(\|x\|) dx \right), & \quad (110)
\end{aligned}$$

We also have

$$\begin{aligned}
\beta &= \lambda(1-p)(1-\nu)2\pi \int_{\mathbb{R}^+} \xi_{\Psi,\Phi}(r) f(r) r dr \\
\eta &= \lambda^2(1-p)p\nu 2\pi \int_{\mathbb{R}^+} \xi_{\Psi,\Phi}(r) f(r) r dr, & \quad (111)
\end{aligned}$$

which is the first moment RCP in this case (the first equation says that the rate of entrance in the susceptible state is the rate of infections that do not lead to death, and the second one that the external birth rate is the total death rate), and

$$\xi_{\Xi,\Xi}(r) = (1-p)^2\xi_{\Psi,\Psi}(r) + p^2\xi_{\Phi,\Phi}(r) + 2p(1-p)\xi_{\Psi,\Phi}(r), \quad (112)$$

which is the conservation equation discussed above. We also have

$$\begin{aligned}
\lambda^2\gamma + \lambda\eta &= \gamma\lambda^2\xi_{\Xi,\Xi}(r) \\
&+ \nu\lambda^2(1-p)^2\xi_{\Psi,\Psi}(r) \int_{\mathbb{R}^2} \mu(\Phi)_{\Psi,\Psi}^{0,r}(x) f(\|x\|) dx \\
&+ \nu\lambda^2(1-p)p\xi_{\Psi,\Phi} \left( f(r) + \int_{\mathbb{R}^2} \mu(\Phi)_{\Psi,\Phi}^{0,r}(x) f(\|x\|) dx \right). & \quad (113)
\end{aligned}$$

This is obtained by balancing the mass birth and death rates in  $\rho_{\Xi,\Xi}^{(2)}$ .

So we have 4 unknown pair correlation functions, 2 unknown parameters ( $\lambda$  and  $p$ ), and 6 equations relating them.

Associated with this model, one can define a functional equation based on any of the Bayes' heuristics discussed above as well as a polynomial equation.



## 8 List of Conjectures

We list here the main conjectures stated in the present paper:

- The repulsion conjecture in Section 4.2;
- The high velocity conjecture in Section 4.3;
- The  $(\mu, \beta)$ -phase diagram in Section 5.5.

The first two conjectures are strongly backed by simulation. The last one is only partly backed by simulation. The three conjectures are mutually compatible: (i) the repulsion vanishes in the high velocity regime; (ii) everywhere in the unsafe region, high velocity leads to survival.

## 9 Appendix

### 9.1 On the Far Random Waypoint Model

In a first step, let us show using the Stein-Chen method to prove:

**Lemma 10.** *Let  $\Phi = \sum_n \delta_{X_n}$  be a stationary point process of intensity  $\lambda$  in  $\mathbb{R}^2$ . If  $\{D_n\}_n$  is a sequence of i.i.d. Gaussian vectors with each vector having independent  $\mathcal{N}(0, \sigma^2)$  entries, then, conditionally on  $\Phi$ ,  $\Psi = \sum_n \delta_{X_n + D_n}$  is approximately Poisson homogeneous of intensity  $\lambda$  in  $\mathbb{R}^2$  when  $\sigma$  is large.*

*Proof.* Let  $A$  be a bounded measurable set of  $\mathbb{R}^2$ . Let us first prove that, when  $\sigma$  is large,  $\Psi(A)$  is approximately Poisson when  $\sigma$  is large. We have

$$\Psi(A) = \sum_n 1_{X_n + D_n \in A}$$

and

$$\mathbb{P}[X_n + D_n \in A \mid \Phi] = \pi_n(\Phi) = \int_A f_\sigma(y - X_n) dy$$

with  $f_\sigma(\cdot)$  the Gaussian density alluded to above. The first observation is that the series  $\sum_n \pi_n(\Phi)$  is a.s. convergent. Indeed,

$$\begin{aligned} \mathbb{E}\left[\sum_n \pi_n(\Phi)\right] &= \int_{\mathbb{R}^2} \lambda dx \int_A f_\sigma(y - x) dy \\ &= \lambda \int_A dy \int_{\mathbb{R}^2} f_\sigma(y - x) dx = \lambda |A|, \end{aligned}$$

where we successively used Campbell's formula, Fubini's theorem, and the fact that the integral of the Gaussian density is 1. Let

$$S(\Phi, A) := \sum_n \pi_n(\Phi).$$

From the Stein-Chen theorem, conditionally on  $\Phi$ , the variation distance between  $\Psi(A)$  and the Poisson law of parameter  $S(\Phi, A)$  is bounded above by

$$2 \sum_n \pi_n^2(\Phi).$$

We now prove that when  $\sigma$  tends to infinity, the last sum tends to 0. We have, with  $x = (x_1, x_2)$  and  $y = (y_1, y_2)$ ,

$$\begin{aligned} \mathbb{E}\left[\sum_n \pi_n^2(\Phi)\right] &= \int_{\mathbb{R}^2} \lambda dx \left( \int_A f_\sigma(y-x) dy \right)^2 \\ &= \int_{\mathbb{R}^2} \lambda dx \left( \int_A \frac{1}{2\pi\sigma^2} e^{-\frac{(y_1-x_1)^2}{2\sigma^2}} e^{-\frac{(y_2-x_2)^2}{2\sigma^2}} dy_1 dy_2 \right)^2 \end{aligned}$$

Using now the fact that

$$\int_A \frac{1}{2\pi\sigma^2} e^{-\frac{(y_1-x_1)^2}{2\sigma^2}} e^{-\frac{(y_2-x_2)^2}{2\sigma^2}} dy_1 dy_2 \leq |A| \frac{1}{2\pi\sigma^2},$$

we get

$$\begin{aligned} \mathbb{E}\left[\sum_n \pi_n^2(\Phi)\right] &\leq \int_{\mathbb{R}^2} \lambda dx |A| \frac{1}{2\pi\sigma^2} \int_A \frac{1}{2\pi\sigma^2} e^{-\frac{(y_1-x_1)^2}{2\sigma^2}} e^{-\frac{(y_2-x_2)^2}{2\sigma^2}} dy_1 dy_2 \\ &= \lambda |A|^2 \frac{1}{2\pi\sigma^2}. \end{aligned} \tag{114}$$

So

$$\lim_{\sigma \rightarrow \infty} \mathbb{E}\left[\sum_n \pi_n^2(\Phi)\right] = 0,$$

which shows that  $\sum_n \pi_n^2(\Phi)$  tends to 0 in  $L1$  when  $\sigma \rightarrow \infty$ . What we want here is almost sure convergence. This follows from the following observation: for all families of non-negative random variables  $Z_k$ , if  $\sum_k \mathbb{E}[Z_k] < \infty$ , then  $Z_k \rightarrow 0$  a.s. as  $k \rightarrow \infty$ . This immediately follows from the fact that  $\sum_k Z_k$  is then a.s. finite. But we get from (114) that

$$\sum_k \mathbb{E}\left[\sum_n \pi_n^2(\Phi, k)\right] < \infty,$$

where  $\pi(\Phi, \sigma)$  is what was denoted by  $\pi(\Phi)$  above and where the dependency in  $\sigma$  was made explicit. Hence

$$\lim_{k \rightarrow \infty} \sum_n \pi_n^2(\Phi, k) < \infty, \quad a.s.$$

The fact that  $\Psi$  is a conditional Poisson point process of intensity measure  $S(\Phi, \cdot)$  follows from the easily proved fact that, conditionally on  $\Phi$ , for all  $A$  and  $B$  bounded and disjoint,  $\Psi(A)$  and  $\Psi(B)$  are independent.  $\square$

The setting is that of the last lemma. We now show:

**Lemma 11.** *Assume in addition that  $\Phi$  is mixing and that its second factorial moment measure admits a density. Then, when  $\sigma$  tends to infinity, (i)  $\Psi$  and  $\Phi$  are asymptotically independent; (ii)  $S(\Phi)$  tends to  $\lambda|A|$ .*

*Proof.* The first property implies the second one since

$$S(\Phi) = \mathbb{E}[\Psi(A) \mid \Phi] = \mathbb{E}[\Psi(A)] = \lambda A.$$

Let us now prove the first one. For all  $A$  and  $B$  bounded, we have

$$\begin{aligned} \mathbb{E}[\Phi(A)\Psi(B)] &= \mathbb{E} \left[ \left( \sum_n 1_{X_n \in A} \right) \left( \sum_m 1_{X_m + D_m \in B} \right) \right] \\ &= \mathbb{E} \left[ \sum_n 1_{X_n \in A} 1_{X_n + D_n \in B} \right] \\ &\quad + \mathbb{E} \left[ \left( \sum_n 1_{X_n \in A} \right) \left( \sum_{m \neq n} 1_{X_m + D_m \in B} \right) \right]. \end{aligned}$$

From Campbell's formula,

$$\begin{aligned} \mathbb{E} \left[ \sum_n 1_{X_n \in A} 1_{X_n + D_n \in B} \right] &= \lambda \int_{x \in A} \int_z f(z) 1_{x+z \in B} dz dx \\ &\leq \lambda |A| |B| \frac{1}{2\pi\sigma^2} \rightarrow_{\sigma \rightarrow \infty} 0. \end{aligned}$$

Let  $c(u)$  denote the pair correlation function of  $\Phi$ . We have

$$\begin{aligned}
\mathbb{E}[\Phi(A)\Psi(B)] &= \mathbb{E}\left[\left(\sum_n 1_{X_n \in A}\right)\left(\sum_{m \neq n} 1_{X_m + D_m \in B}\right)\right] \\
&= \int_{x \in A} \int_y \int_z f(z) 1_{y+z \in B} \lambda^2 c(x-y) dx dy dz \\
&= \int_{x \in A} \lambda dx \int_y c(x-y) dy \int_{t \in B} f(t-y) \lambda dt \\
&= \int_{x \in A} \lambda dx \int_{t \in B} \lambda dt \int_y c(x-y) f(t-y) dy.
\end{aligned}$$

But for all fixed  $x$  and  $t$ ,

$$\int_y c(x-y) f(t-y) dy = \int_y c(u-t+x) f(u) du = \mathbb{E}[c(D_\sigma - t + x)],$$

with  $D_\sigma$  a Gaussian random variable as above. To analyze the limiting behavior of the last expression, consider the coupling  $D_\sigma = \sigma D$ . Using the dominated convergence theorem,

$$\lim_{\sigma \rightarrow \infty} \mathbb{E}[c(D_\sigma - t + x)] = \lim_{\sigma \rightarrow \infty} \mathbb{E}[\lim_{\sigma \rightarrow \infty} c(D_\sigma - t + x)] = 1.$$

The fact that  $\lim_{\sigma \rightarrow \infty} c(D_\sigma - t + x) = 1$  a.s. follows from the mixing assumption. Using this and once more the dominated convergence theorem

$$\begin{aligned}
\lim_{\sigma \rightarrow \infty} \mathbb{E}[\Phi(A)\Psi(B)] &= \lim_{\sigma \rightarrow \infty} \int_{x \in A} \lambda dx \int_{t \in B} \lambda dt \mathbb{E}[c(D_\sigma - t + x)] \\
&= \int_{x \in A} \lambda dx \int_{t \in B} \lambda dt \lim_{\sigma \rightarrow \infty} \mathbb{E}[c(D_\sigma - t + x)] \\
&= \lambda|A|\lambda|B| = \mathbb{E}[\Phi(A)]\mathbb{E}[\Psi(B)].
\end{aligned}$$

□

The properties mentioned at the end of Subsection 3.2 are obtained in the same way as above and are outlined below.

- Let  $\{\Phi_t\}_t$  and  $\{\Psi_t\}$  be the steady state processes of the infected and susceptible points. Let  $\lambda p$  and  $\lambda(1-p)$  denote their intensities.
- Let  $t < u$  be fixed. Let  $\Xi_k$ ,  $k \geq 1$ , be sub-point process of  $\Phi_t$  which have  $k$  jumps in  $[t, u]$ ;

- Let  $\tilde{\Phi}_k$  denote the displaced points of  $\Phi_k$ ; by the arguments of the last two lemmas,  $\tilde{\Phi}_t$  is approximately a Poisson point process of intensity  $\lambda p q(\gamma(u-t), k)$  with  $q(\gamma(u-t), k)$  the probability that a Poisson random variable of parameter  $\gamma(u-t)$  is equal to  $k$ . The point processes  $\tilde{\Phi}_k$  are independent, so that the "infected arrival" point process  $\mathcal{I} = \sum_{\parallel} \tilde{\Phi}$  in this interval is Poisson of intensity  $\lambda p \gamma(u-t)$ ;
- By the same argument, the "susceptible arrival" point process  $\mathcal{S}$  in this interval is Poisson of intensity  $\lambda(1-p)\gamma(u-t)$ ;
- The point processes  $\mathcal{I}$ ,  $\mathcal{S}$ , and  $(\Phi_u, \Psi_u)$  are independent.

## 9.2 On the Boolean Cluster above Percolation

First, we recall some classical results from [9]. For a Poisson point process of intensity  $\lambda$  in  $\mathbb{R}^2$ , the Boolean model of radius  $a$  percolates for  $\mu = \lambda \pi a^2 > \mu_c$ , with  $\mu_c \sim 4.5$ . That is, if  $\lambda = 1$ , the model percolates for  $a > a_c \sim 1.2$ . If  $a = 1$  the model percolates for  $\lambda > \lambda_c = 1.4$ .

Consider the Poisson point process  $\tilde{\Xi}$  of intensity  $\tilde{\lambda}$  under its double Palm distribution at 0 and  $R = (0, r)$ . Consider the Boolean model with radius  $a$  on  $\Xi$ . Let  $\pi(r)$  denote the probability that 0 and  $R$  are connected. When denoting by  $x \sim y$  the event that  $x$  and  $y$  are connected, we have

$$1 - \pi(r) = \mathbb{P}(\cap_{i: X_i \in B(0, a)} \{X_i \sim R\})^c.$$

Under the approximation stating that the events  $\{X_i \sim R\}$  are conditionally independent given  $\Xi \cap B(0, a)$ , with respective probabilities  $\pi(\|X_i - R\|)$ , we get

$$\pi(r) = 1 - \exp\left(-\lambda \int_{v=0}^a \int_{\theta=0}^{2\pi} \pi\left(\sqrt{r^2 + v^2 + 2rv \cos(\theta)}\right) v dv d\theta\right), \quad r > a,$$

with  $\pi(r) = 1$  for  $r \leq a$ . For  $r$  large, we get that  $q = \pi(\infty)$  solves the Lambert equation

$$q = 1 - \exp(-\tilde{\mu}q), \tag{115}$$

which is also the equation for the probability of survival of a branching process with Poisson progeny of parameter  $\tilde{\mu} = \tilde{\lambda} \pi a^2$ . This equation has no positive solution when  $\tilde{\mu} < 1$  and a single solution  $q_{\tilde{\mu}}$  in  $(0, 1)$  for  $\tilde{\mu} > 1$ , which can be interpreted as the probability of survival. In contrast the probability of extinction (of the branching process) is  $1 - q_{\tilde{\mu}}$ . It follows that, in this approximation, the density of points that lie in finite clusters is  $1 - q_{\tilde{\mu}}$  so that the intensity of the infinite

cluster (seen as a stationary point process  $\Xi$ ) is  $q_{\bar{\mu}}$ . This leads to the following approximation for the pair correlation function of  $\Xi$ :

$$\xi_{\Xi, \Xi}(r) = \frac{\pi(r)}{q_{\bar{\mu}}}. \quad (116)$$

In particular, in this approximation

$$\xi_{\Xi, \Xi}(r) = c_{\bar{\mu}} := \frac{1}{q_{\bar{\mu}}}, \quad \forall r < a. \quad (117)$$

### 9.3 Mean Time between Two Infections

Let  $\nu$  be the mean time between infections of an individual. Now consider the queue of healthy individuals. Then Little's Law yields:

$$\begin{aligned} \lambda(1-p) &= \lambda p \beta \nu \\ \implies \nu &= \frac{1-p}{p\beta} \end{aligned} \quad (118)$$

**Acknowledgements** The authors would like to thank Charles Radin and Fabien Mathieu for their valuable suggestions on this preprint. F. Baccelli was supported by the ERC NEMO grant, under the European Union's Horizon 2020 research and innovation programme, grant agreement number 788851 to INRIA.

## References

- [1] F. Baccelli., B. Blaszczyzyn, and M. Karray, *Random Measures, Point Processes, and Stochastic Geometry*, Online book preprint, 2020, <https://hal.inria.fr/hal-02460214>
- [2] F. Baccelli, F. Mathieu, and I. Norros, "On Spatial Point Processes with Uniform Births and Deaths by Random Connection", *Queueing Syst.* 86(1-2): 95-140, 2017.
- [3] B. Blaszczyzyn, C. Rau, and V. Schmidt. "Bounds for clump size characteristics in the Boolean model", *Advances in Applied Probability*, (310)-4: 910–928, 1999.
- [4] T. Liggett, *Stochastic Interacting Systems*, Springer, 1999.

- [5] D. Figueiredo, G. Iacobelli, and S. Shneer, “The End Time of SIS Epidemics Driven by Random Walks on Edge-Transitive Graphs”, *Journal of Statistical Physics*, (179)-3: 651–671, 2020.
- [6] R. Pastor-Satorras, C. Castellano, P. Van Mieghem, and A. Vespignani “Epidemic processes in complex networks.” *Rev. Mod. Phys.* 87(3), 925, 2015.
- [7] R. Pemantle, “The contact process on trees.” *Ann. Probab.*, 20 (4), 2089–2116, 1992.
- [8] A. Sankararaman, F. Baccelli, and S. Foss, “Interference Queueing Networks on Grids”, *Annals of Applied Probability*, 29(5): 2929-2987, 2019.
- [9] D. Stoyan, W. Kendall, and J. Mecke, *Stochastic Geometry and its Applications*, Wiley, 1995.
- [10] C. V. Hao, “Super-exponential extinction time of the contact process on random geometric graphs.” *Combinatorics, Probability and Computing* 27.2 (2018): 162-185.
- [11] G. Ganesan, “Infection spread in random geometric graphs.” *Advances in Applied Probability* 47.1 (2015): 164-181.
- [12] L. Ménard and A. Singh, “Percolation by cumulative merging and phase transition for the contact process on random graphs.” *arXiv preprint arXiv:1502.06982* (2015).
- [13] M. E. J. Newman, “*Networks.*” Oxford University Press, 2018.